NPS67-82-13

NAVAL POSTGRADUATE SCHOOL

Monterey, California

AN INVESTIGATION OF THE EFFECTIVENESS OF SMOKE SUPPRESSANT FUEL ADDITIVES FOR TURBOJET APPLICATIONS

John R. Bramer and David W. Netzer

September 1982

Prepared for:

Naval Air Propulsion Center
Trenton, NJ 08600

NAVAL POSTGRADUATE SCHOOL
Monterey, California

Rear Admiral J. J. Ekelund
Superintendent

D. A. Schrady
Provost

The work reported herein was supported by the Naval Air Propulsion Center, Trenton, New Jersey, as part of the Naval Environmental Protection Technology Program.

This report was prepared by:

DAVID W. NETZER
Professor
Department of Aeronautics

Reviewed by:

D. M. LAYTON
Acting Chairman
Department of Aeronautics

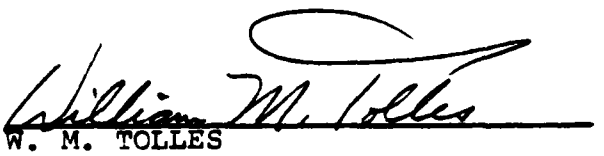

W. M. TOLLES
Dean of Research

UNCLASSIFIED

SECURITY CLASSIFICATION OF THIS PAGE (When Data Entered)

RMS REPORT DOCUMENTATION PAGE	READ INSTRUCTIONS BEFORE COMPLETING FORM
1. REPORT NUMBER: NPS67-82-13 — 2. GOVT ACCESSION NO.: AD-A112228	3. RECIPIENT'S CATALOG NUMBER:
4. TITLE (and Subtitle): AN INVESTIGATION OF THE EFFECTIVENESS OF SMOKE SUPPRESSANT FUEL ADDITIVES FOR TURBOJET APPLICATIONS	5. TYPE OF REPORT & PERIOD COVERED: Final 1982
	6. PERFORMING ORG. REPORT NUMBER:
7. AUTHOR(s): John R. Bramer, David W. Netzer	8. CONTRACT OR GRANT NUMBER(s): N6237681WR00014
9. PERFORMING ORGANIZATION NAME AND ADDRESS: Naval Postgraduate School, Monterey, California 93940	10. PROGRAM ELEMENT, PROJECT, TASK AREA & WORK UNIT NUMBERS:
11. CONTROLLING OFFICE NAME AND ADDRESS: Naval Air Propulsion Center, Trenton, New Jersey 08628	12. REPORT DATE: September 1982
	13. NUMBER OF PAGES: 61
14. MONITORING AGENCY NAME & ADDRESS(if different from Controlling Office): Naval Postgraduate School, Monterey, California 93940	15. SECURITY CLASS. (of this report): UNCLASSIFIED
	15a. DECLASSIFICATION/DOWNGRADING SCHEDULE:

16. DISTRIBUTION STATEMENT (of this Report)

Approved for public release; distribution unlimited

17. DISTRIBUTION STATEMENT (of the abstract entered in Block 20, if different from Report)

18. SUPPLEMENTARY NOTES

19. KEY WORDS (Continue on reverse side if necessary and identify by block number)

Turbojet
Test Cell
Pollution
Fuel Additives

20. ABSTRACT (Continue on reverse side if necessary and identify by block number)

Seven fuel additives were tested to investigate their effectiveness at reducing exhaust stack gas opacity in a turbojet test cell. Exhaust particle sizes and mass concentrations were determined at the engine and stack exhausts using measurements of light transmittance at three frequencies. Particle samples were also collected at the engine exhaust and measured with a scanning electron microscope to verify the optical technique.

DD FORM 1 JAN 73 1473 EDITION OF 1 NOV 65 IS OBSOLETE
S/N 0102-LF-014-6601

UNCLASSIFIED
SECURITY CLASSIFICATION OF THIS PAGE (When Data Entered)

20. Abstract (continued)
Nitrous oxide emissions were measured at the test cell stack exhaust.

Four of the additives tested were found effective at reducing stack exhaust opacity and particulate mass concentration. None of the additives had any measurable effect on particle diameters. No meaningful changes in particle size or mass occurred between the engine and stack exhausts. The optical technique for determining particle size was verified effective using the scanning electron microscope. No additive had any significant effect on nitrous oxide production.

TABLE OF CONTENTS

A

LIST OF TABLES

LIST OF FIGURES

TABLE OF SYMBOLS AND ABBREVIATIONS

AUG. RATIO	Augmentation ratio
C_{m_e}	Engine exhaust particulate mass concentration ($\times 10^{-6}$ gm./liter gas)
C_{m_s}	Stack exhaust particulate mass concentration ($\times 10^{-6}$ gm./liter gas)
d_{32}	Volume-to-surface mean particle diameter (microns)
$\left[\frac{f}{a}\right]_p$	Fuel to air ratio (primary air): $\dot{m}_f/\dot{m}_p$
$\left[\frac{f}{a}\right]_{p+s}$	Fuel to air ratio (primary + secondary air): $\dot{m}_f/\dot{m}_e$
m	Complex refractive index
$\dot{m}_{aug.\ t.}$	Augmentor tube mass flow rate (lbm/sec.)
$\dot{m}_{BP}$	Bypass air mass flow rate (lbm/sec.)
$\dot{m}_{c_e}$	Particulate mass flow rate at the engine exhaust (gm./sec.)
$\dot{m}_{c_s}$	Particulate mass flow rate at the stack exhaust (gm./sec.)
$\dot{m}_e$	Engine air mass flow rate ($\dot{m}_p + \dot{m}_s$) (lbm/sec.)
$\dot{m}_{e_T}$	Total engine air mass flow rate ($\dot{m}_{BP} + \dot{m}_e$) (lbm/sec.)
$\dot{m}_f$	Fuel mass flow rate (lbm/sec.)
$\dot{m}_p$	Combustor primary air mass flow rate (lbm/sec.)
$\dot{m}_s$	Combustor secondary air mass flow rate (lbm/sec.)

NO_x	Nitrogen oxide concentration; parts per million (PPM), non-calibrated
T_λ	Percent transmittance at wavelength λ
T_{BP}	Bypass air temperature (°R)
T_C	Combustor exhaust temperature at combustor exit (°R)
T_{mix}	Bulk temperature of the fuel/air mixture at the engine exhaust (°R)
T_R	Gas stagnation temperature at the stack end of the augmentor tube (°R)
σ	Geometric standard deviation

I. INTRODUCTION

All organizations tasked with the maintenance of modern high performance turbojet/turbofan engines utilize jet engine test cells as a means of monitoring engine performance. The Navy uses test cells at its various jet engine rework facilities to statically achieve in a controlled environment the full range of operating conditions to which a repaired engine will eventually be subjected. All engines are thus fully tested prior to being placed back into service. This results in both lowering the number of engines that fail in flight and raising the degree of safety involved with the entire repair process.

The federal Environmental Protection Agency (EPA) issues minimum national pollution control guidelines which may subsequently be made more stringent by local governmental regulation. Military jet engines which are exempt from these various pollution control requirements while operating installed in aircraft must, however, conform to all regulations, federal and local, while being evaluated in a test cell. Such local standards imposed by the San Diego and Bay Area Regional Air Quality Districts have resulted in lawsuits against the Navy [Ref. 1].

Of primary concern in these local pollution requirements is the test cell exhaust resulting from the engines being

evaluated. Since the purpose of the test cell is to simulate as closely as possible the actual flight environment, the problem then is how to meet the local pollution standards while maintaining the validity of the tests.

While future technology may in time be able to produce nearly pollution-free, high-performance aircraft engines, there will remain literally thousands of older engines in service requiring periodic test cell evaluation. An interim means of controlling the large amounts of smoke emitted during these tests is required. Additionally a reduction in the amount of nitrogen oxides being produced would be beneficial. One possible means of reducing the smoke being released into the atmosphere is the modification of existing test cells. This solution at present appears to be very expensive and difficult to achieve while maintaining the proper engine testing environment. The effectiveness of various fuel additives has also been investigated as a possible inexpensive solution to this problem.

Research documented in this thesis is a culmination of the efforts of five previous aeronautical engineering students at the Naval Postgraduate School. Hewlett [Ref. 2] initiated the program with design and construction of a one-eighth scale turbojet test cell at the school's Aeronautics Laboratory. Charest [Ref. 3] designed, constructed, and evaluated the use of a ramjet type dump combustor for simulation of the turbojet combustion process. In another

research program, Hewett [Ref. 4] utilized light extinction measurements to determine the effects of fuel composition and bypass ratio on the concentration and size of unburned carbon within a solid fuel ramjet. Darnell [Ref. 5] adapted the latter technique to make measurements of particle sizes and concentrations in the sub-scale test cell. His efforts were partially successful and resulted in recommendations for improvements in the experimental techniques in order to improve the quality of collected data. Thornburg [Ref. 6] incorporated these suggestions and used the improved facility for experiments to investigate the overall effectiveness of several smoke suppressant fuel additives.

A large number of smoke suppressant fuel additives have been developed by various manufacturers. Some of these have been evaluated by the Naval Air Propulsion Test Center [Ref. 7] for their effectiveness in reducing the smoke produced by turbojet engines. Ferrocene and DGT-2 were found to be effective.

Previous research has indicated that the additives most effective at reducing test cell exhaust plume opacity are metallic based. Ferrocene solution in particular [Refs. 8 and 9] has been very effective. However, there is some concern that engines with very high turbine inlet temperatures may be susceptible to a build-up of iron deposits on the turbine blades, due to the relatively low melting temperature of the iron. Thus, there is a need to determine if some of the

rare earth metals (such as cerium), with their higher melting temperatures, can be as effective in a fuel additive solution as the ferrocene.

The exact process by which particulates are formed in the turbojet combustion process is not entirely understood. The particulate matter has been estimated to be approximately 96% carbon by weight [Ref. 10]. Light is scattered and absorbed by the particulates so that the plume opacity is related to their size and concentration [Ref. 11]. It is not clear how these properties are altered by the test cell and by the use of fuel additives. Particulates may be altered within the combustor, and/or after they leave the combustor by dilution from bypass air in the engine, by dilution in the augmentor tube, or by mixing and cooling in the stack prior to exiting to the atmosphere.

Previous research conducted at the Naval Postgraduate School [Ref. 11] evaluated Ferrocene, 12% Rare Earth Hex-Cem, and 12% Cerium Hex-Cem in varying concentrations to determine their effects on engine and stack exhaust opacities and particulate mean diameters. Thornburg showed Ferrocene and 12% Cerium Hex-Cem both effectively reduced stack exhaust opacity between thirty and forty percent for additive concentrations between twenty and thirty milliliters per gallon of JP-4. 12% Rare Earth Hex-Cem was ineffective as a smoke suppressant additive. It was noted that exhaust gas opacity was very

sensitive to combustor exhaust temperature (primary fuel-air ratio).

Throughout these previous investigations at NPS, particulate volume to surface mean diameter (d_{32}) varied between .18 and .24 microns, with an average of about .21 microns. This range was not considered a significant change in average particle diameter, thus it was concluded that the particle diameters remained essentially constant throughout all tests and that varying additive concentrations had no significant effect on d_{32}. The data also indicated that no variations in particle diameter occurred between the engine exhaust and the stack exhaust.

Fuel additives and increased engine operating temperature decreased the mass concentration of exhaust particulates. A decrease in mass concentration between the engine exhaust and stack exhaust was due primarily to dilution of the engine exhaust gases within the augmentor tube. It was further noted that the fuel additives were most effective for combustor exhaust gas temperatures of 1450°F or higher, and that none of the additives produced any significant change in NO_x concentrations at the stack exhaust.

Based upon the work done previously by Darnell, Thornburg, and Netzer [Refs. 5, 6, and 11] some modifications to the testing apparatus and in the experimental technique were made. The narrow bandpass light filters used in the light transmission equipment were changed at the engine exhaust

location to match the frequencies of those used at the test cell stack exhaust. This was done to remove one possible ambiguity from the later evaluation of collected data.

It was also observed in previous testing that, due to the water cooling jacket surrounding the combustor, soot was building up quite rapidly on the walls of the primary combustor. Therefore, in order to standardize the testing for all additives, the combustor was completely disassembled, cleaned, and reassembled for each test series. This precluded the possibility of soot from one run interfering with the data set from another.

Finally to improve the comparison of data from the various additives, it was necessary to reduce the previously reported large effect that temperature variation had on exhaust stack gas opacity. An effort was made to keep the combustor exhaust temperature as constant as possible within a given test and from run to run. Air flows were also kept as constant as possible from run to run.

Tests during the present investigation were conducted using Ferrocene, 12% Rare Earth Hex-Cem, 12% Cerium Hex-Cem, CV-100, XRG, DGT-2, and 12% Cerium Octotate. This investigation was primarily concerned with determining the effects of various fuel additives on the concentration and size of soot particles at the engine and test cell exhausts. Measurements were made using a three-frequency light transmission technique. Additionally, exhaust particulates were collected and

measured with a scanning electron microscope (SEM) as a means of verifying the optical technique. Opacity of the test cell exhaust was continuously monitored electronically and periodic measurements of nitrous oxide (NO_x) gas were made.

II. EXPERIMENTAL APPARATUS

The sub-scale turbojet test cell and associated supplemental testing equipment used to carry out this investigation have been thoroughly described in several previous reports [Refs. 2, 3, 4, 5, 6, and 11]. A brief recapitulation of the apparatus is made here for report clarity.

A one-eighth (in linear dimensions) scale model of an Alameda Naval Air Station test cell was used to carry out this investigation [Ref. 12]. Figures 1, 2, and 3 show the test cell and its basic plumbing arrangement. Flow straightened air was provided to the visual test section through a horizontal inlet. The augmentor tube exited the cell through a removable wall and dumped the exhaust into a vertical stack.

High pressure air was provided to an externally mounted combustor from a large-volume positive displacement compressor. Four air flows (combustor primary and secondary, motor bypass, and "engine inlet" suction) were remotely controlled to provide the desired values.

The ramjet type dump-combustor used to simulate a turbojet engine is illustrated in Figs. 4 and 5 and described in detail in Ref. 3. By varying the primary fuel/air ratio and secondary air flow, the exhaust temperature and particulate

concentration (i.e. opacity) could be altered. The combustion was water cooled for chamber wall protection.

The fuel system consisted of a remotely controlled, seven gallon capacity, portable fuel supply and two Eldex, Model E, precision metering pumps for fuel additive injection. Fuel flow rate to the combustor was controlled by a cavitating venturi installed in the fuel line and by varying the pressure of gaseous nitrogen in the fuel tanks. A calibration curve for fuel flow rate versus pressure using a .017 in. venturi is shown in Fig. 6. The Eldex precision metering pumps are shown in Fig. 7. Figure 8 presents the calibrated metering pump flow rates versus pump micrometer settings.

Using standard ASME flow calculations [Ref. 13], automatic data acquisition of test cell temperatures and pressures, and data processing of test cell mass flows, were provided on demand by an HP-21 MX computer system. A permanent record of temperatures, pressures, flow rates, and other data of interest was made via the computer's hard copy printer. Additionally a continuous record of combustor exhaust temperature was made using a strip chart recorder.

A Leads and Northrop model 6597 transmissometer was set up to provide a direct read-out of test cell stack exhaust stream opacity. Figure 9 shows the source and detector and Fig. 10 shows the signal conditioner/display unit. A continuous record of stack exhaust opacity was kept using a strip chart recorder.

Engine and stack exhaust particle sizes were measured using a three frequency light transmission technique. The equations used to reduce the run data recorded on strip chart recorders are presented in Refs. 6, 12, 14, and 15. To verify the optically obtained data, exhaust particulate samples were collected at the engine exhaust [Fig. 11] and the particle sizes measured with a scanning electron microscope.

Finally, test cell stack exhaust gas was sampled to determine the effect of fuel additives on NO_x production. The probe shown in Fig. 9 was connected to a Monitor Labs, Model 8440E, Nitrogen Oxides Analyzer shown in Fig. 12 and described in Ref. 16.

III. EXPERIMENTAL PROCEDURE

The fuel additives tested in this investigation were run at their optimum concentrations as determined by Thornburg, Darnell, and Netzer [Ref. 11]. Those additives not previously evaluated were run with either the manufacturer's recommended concentration or with a concentration equal to that employed for one of the other additives. In some cases additional concentrations were also used to compare with the results obtained using the nominal values.

Every additive test series was started with a clean combustor. The optical detector systems and the transmissometer were checked and zeroed. When all the measurement equipment was calibrated, air flow rates were adjusted to obtain the following nominal values:

Combustor primary air - - - - - - - - - -	.286 (lbm/sec)
Combustor secondary air - - - - - - - - -	.228 (lbm/sec)
3 inch bypass line air - - - - - - - - -	.900 (lbm/sec)
6 inch suction line air - - - - - - - - -	1.040 (lbm/sec)

These settings would change somewhat with motor ignition.

With air flowing through the motor and test cell, a final check of the measurement equipment was made. New zeros and one hundred percent readings were taken as necessary. After all final adjustments were complete, the fuel tank/cavitating venturi pressure was adjusted to obtain the desired fuel flow

rate (Fig. 6). An oxygen/ethylene ignition torch was used to ignite the JP-4 fuel-air mixture in the combustor.

Combustor exhaust temperature was kept as close to 1530°F as possible. Tests in which this temperature was maintained between 1500 and 1600°F were considered acceptable based upon the previous results of Thornburg et al [Ref. 11]. This temperature range was maintained by making small changes in the JP fuel flow rate.

For the remainder of each test, the fuel additive being evaluated would be turned on and off several times until sufficient steady-state data were collected. Values for combustor exhaust temperature, fuel tank pressure, venturi pressure, NO_x concentration, fuel additive flow rate, exhaust stack opacity, and combustor inlet pressure were visually observed and recorded. Opacity, combustor exhaust temperature, and the six light transmittances were continuously recorded on strip chart recorders. Test cell air mass flow rates, temperatures, and test cell augmentation ratio were recorded on demand by the HP-21 MX computer. Particulate samples were collected during each test, both with and without fuel additives being turned on.

When data collection was complete the JP fuel was turned off, but the air flows were kept running in order to provide rapid cool-down of the combustor and to purge any unburned JP fuel. Post-run calibrations were made to ensure that the zeros and one hundred percent readings had not changed. Test

cell air mass flows were also checked to ensure that they returned to their pre-run nominal settings.

IV. DATA REDUCTION

A. OPACITY

Opacity of the test cell stack exhaust gases was measured directly with a white light source transmissometer. As defined by the EPA, opacity is the degree to which emissions reduce the transmission of light and obscure the view of an object in the background [Ref. 17]. Opacity is related to the transmittance of light by:

$$\% \text{ OPACITY} = 100\% - \% \text{ TRANSMITTANCE.}$$

B. PARTICULATE SIZE

Exhaust particulates were measured at the engine and stack exhausts using Bouguer's Law [Ref. 14] for the transmission of light through a cloud of uniform particles:

$$T = \exp(-QAnL) = \exp\left[-(3QC_m L/2\rho d)\right] \qquad (1)$$

where (T) is the fraction of light transmitted, (Q) is the dimensionless extinction coefficient, (A) is the cross sectional area of a particle, (n) is the number concentration of particles, (L) is the path length the light beam traverses, (C_m) is the mass concentration of particles, (ρ) is the density of an individual particle, and (d) is the particle diameter.

Using Mie light scattering theory, the dimensionless extinction coefficient (Q) can be calculated as a function of particle size, wavelength of light, and complex refractive index of the particle.

Dobbins [Ref. 15] revised Bouguer's transmission law to allow for a distribution of particle sizes:

$$T = \exp\left[-\left(3\bar{Q}C_m L/2\rho d_{32}\right)\right] \tag{2}$$

where $(\bar{Q})$ is an average extinction coefficient and (d_{32}) is the volume-to-surface mean particle diameter. Taking the natural logarithm of equation (2):

$$\ln[T] = \bar{Q}\left[-3C_m L/2\rho d_{32}\right]. \tag{3}$$

For a specific wavelength of light, equation (3) can be written:

$$\ln[T_\lambda] = \bar{Q}_\lambda\left[-3C_m L/2\rho d_{32}\right]. \tag{4}$$

Assuming C_m, L, ρ, and d_{32} remain constant, the ratio of the natural logs of the transmittances for two wavelengths of light is:

$$\frac{\ln[T_{\lambda 1}]}{\ln[T_{\lambda 2}]} = \frac{\bar{Q}_{\lambda 1}}{\bar{Q}_{\lambda 2}} \cdot \tag{5}$$

A Mie scattering computer program, provided by K. L. Cashdollar of the Pittsburgh Mining and Safety Research Center, Bureau of Mines, produced calculations of $\bar{Q}_\lambda$ and $\bar{Q}_\lambda$ ratios as

a function of d_{32}. The following inputs to that program were used for this investigation:

Complex Refractive Index of Particles (m = 1.95 - .66i)

Refractive Index of Surrounding Medium (1.0 for air)

Standard Deviation of the Distribution (σ = 2.0)

Three Wavelengths of Light (4500 Å, 6500 Å, 10140 Å)

Transmissivity was determined by comparing the ratios of photodiode outputs with and without exhaust particles present (i.e. combustor on and off respectively). d_{32} and $\bar{Q}_\lambda$ were obtained from the output of Cashdollar's program (Figs. 13 and 14) using the log ratios of transmissivity of the three wavelengths of light measured at both engine and stack exhausts. Using three transmittance ratios provides three values for d_{32}. If all three d_{32} values are not nearly identical, then the complex refractive index and/or standard deviation chosen are not correct [Ref. 14]. Several values of m (complex refractive index) and σ (standard deviation) were used in the study. The set providing the most consistent values of d_{32} were m = 1.95 - .66i and σ = 2.0. Once $\bar{Q}_\lambda$, d_{32}, and T_λ were known, mass concentration was calculated with the following rearrangement of equation (4):

$$C_m = -\frac{2}{3}\left[\frac{\rho d_{32}}{\bar{Q}_\lambda L}\right] \ln T_\lambda. \qquad (6)$$

C. PARTICULATE MASS FLOW

Previous research by Thornburg et al [Ref. 11] showed a significant decrease in particulate mass concentration between the engine and stack exhausts. The particulate mass flow rates can be written:

$$\dot{m}_{c_e} = C_{m_e} Q_e \tag{7}$$

$$\dot{m}_{c_s} = C_{m_s} Q_s \tag{8}$$

where Q is the volume flowrate. Assuming perfect gases:

$$Q = AV = \frac{\dot{m}RT}{P} \tag{9}$$

The following assumptions were made for these calculations:

$$R = R_{air} = 53.3 \text{ ft-lbf/lbm-}^\circ R$$

$$P = P_{engine} = P_{stack} = 14.7 \text{ psi}$$

$$\dot{m}_{engine} = \dot{m}_{e_T} = \dot{m}_p + \dot{m}_s + \dot{m}_{BP}$$

$$\dot{m}_{st} = \dot{m}_{stack} = \dot{m}_{augmentor\ tube}$$

$$T_{stack} = T_R$$

$$T_{engine} = T_{mix} = \frac{\dot{m}_{BP} T_{BP} + \dot{m}_e T_c}{\dot{m}_{e_T}}$$

The particulate mass flow rates were then ratioed:

$$\frac{\dot{m}_{ce}}{\dot{m}_{cs}} = \frac{C_{m_e} Q_e}{C_{m_s} Q_s} = \frac{C_{m_e} \dot{m}_e T_{mix}}{C_{m_s} \dot{m}_{st} T_R} \tag{10}$$

A ratio of 1.0 would indicate no change in particulate mass flow rates between the engine and stack exhausts, within the limits of the above approximations. Any decrease in mass concentration at the stack would then be due to dilution of the exhaust particles with augmentation air.

V. RESULTS AND DISCUSSION

A. INTRODUCTION

From April to July of 1982, seven smoke suppressant fuel additives were tested to determine their effects on test cell stack exhaust gas opacity, on d_{32}, on exhaust particulate mass concentrations, and on NO_x concentration. The additives are listed with their respective manufacturers in Table I. Tables II through VIII summarize the data collected and reduced during this investigation.

As mentioned previously, in the NPS test apparatus combustor exhaust temperature and run time were found to greatly influence exhaust stack opacity independent of other variables. Figure 15 shows the effect of combustor exhaust temperature on opacity for a clean combustor. The effect of run time (starting at time zero with a clean combustor) on opacity for this particular combustor is demonstrated in Fig. 16. To minimize these effects between tests with the different additives, data points selected for reduction had a combustor exhaust temperature from 1966 to 2007°R, and a total combustor run time of 20 minutes or less. With these restraints, coupled with fairly constant air mass flows and fuel flows, any changes in opacity, etc. should have been primarily due to the fuel additive being examined.

Figures 17 through 20 show a typical set of strip chart recordings from which the presented data were reduced. Sample SEM photographs of collected exhaust particulates (used to confirm optical d_{32} measurements) are enclosed as Figs. 21 and 22.

B. ADDITIVE EFFECTS ON STACK GAS OPACITY

Tables II through VIII present the data obtained for stack exhaust gas opacities. 12% Rare Earth Hex-Cem, CV-100, and XRG were ineffective in reducing stack gas opacity. Ferrocene, DGT-2, and 12% Cerium Hex-Cem were all tested at concentrations of approximately 28 ml./gal. of JP-4. Ferrocene lowered opacity between twelve and twenty-four percent, DGT-2 between twenty-four and thirty percent, and 12% Cerium Hex-Cem between twenty-one and thirty-five percent. 12% Cerium Octotate was tested at a lower concentration of 22 ml./gal. of JP-4 and reduced the opacity between eleven and nineteen percent.

The latter additive (12% Cerium Octotate) was added to the investigation at the end of the study. Pump settings for this additive were therefore made identical to those used for the 12% Cerium Hex-Cem. However, it was somewhat more viscous than the Hex-Cem which resulted in the tests being conducted at a lower concentration than planned. The Eldex precision metering pumps could pump the Hex-Cem at a maximum flow of 5.5 milliliters per minute versus a maximum of only

3.7 for the Cerium Octotate. The lower additive concentration could have been partially responsible for it being less effective than the 12% Cerium Hex-Cem. However, previous data obtained by Thornburg [Ref. 6] indicated that 12% Cerium Hex-Cem was nearly equally effective for concentrations between 15 and 40 ml./gal. of JP-4.

C. ADDITIVE EFFECTS ON d_{32}

Part B of section IV of this report outlines the optical (three frequency extinction) technique used to calculate d_{32}. The individual test run values of transmittance and d_{32} are listed in tables II through VIII. When the optical technique (using various values of m and σ) resulted in three values of d_{32} within ±.02 microns, that value of d_{32} was deemed acceptable.

Individual values of d_{32} varied from .13 to .28 microns throughout this investigation. However, on any given run this range was much narrower, with a typical variation of only .02 to .03 microns. Given the inaccuracies in measuring the individual transmittance values, this range was considered an insignificant change in average particle diameter. Therefore it was concluded that the additives tested had no significant effect on d_{32}. Also, no significant changes in mean particle diameter occurred between the engine and the stack exhausts.

Table IX compares the optically measured values of d_{32} at the engine exhaust to the range in diameters obtained from SEM photographs (Figs. 21 and 22) of collected particulate samples. The range of sizes observable with the SEM consistently surrounded the values of d_{32} found optically. It therefore appears the optical technique was a reasonably good method for measuring engine exhaust particulate size.

D. ADDITIVE EFFECTS ON MASS CONCENTRATION

Assuming a soot particle density (ρ) of 1.5 gm/cm^3, equation 6 was used to calculate particulate mass concentrations at the engine and stack exhausts. Section IV outlines the mass concentration calculation method.

Equation 6 also requires an input for the path length that the light beam traverses (L). At the engine exhaust L was .0498 meters and at the stack exhaust it was .762 meters. The determinations of mass concentration were somewhat less accurate than those for d_{32} because both ρ and $\bar{Q}$ are rather uncertain in value. Tables II through VIII list the calculated mass concentrations at the stack and engine exhausts for a wavelength of 10140 Angstroms. The mass concentrations calculated at the other frequencies did not vary significantly from these values and are not included.

Ferrocene, DGT-2, 12% Cerium Hex-Cem, and 12% Cerium Octotate all appeared to reduce the mass concentration of soot particles when they were in use. 12% Rare Earth Hex-Cem,

CV-100, and XRG were virtually ineffective in mass concentration reduction.

The particulate mass flows at the engine and stack were ratioed using equation 10 of section IV to determine if the decrease in mass concentrations between the engine exhaust and the stack were due to chemical reactions or wall depositions downstream of the engine exhaust or to flow dilution by augmentation air. Within the approximations made in equation 10, a ratio of 1.0 would indicate no change in particulate mass flow rates between the engine and stack exhausts. Tables II through VIII present these ratios for the data reduced. The ratios varied from a low of 1.1 to a high of 3.2 with an average of approximately 1.5. This would indicate that some chemical reactions or wall deposition involving the particulates occurred between the engine and stack exhausts. However, the light transmission measurements at the stack exhaust were made near the stack centerline. Visual observation of the stack exhaust indicated that it was concentrated to the aft portion of the stack. This observation together with the lack of change in d_{32} indicate that little if any chemical reaction/deposition occurred.

E. ADDITIVE EFFECTS ON NO_x CONCENTRATION

Values of NO_x for the various test runs, with and without additives turned on, are listed in Tables II through VIII. No additive produced a significant change in the NO_x concentration on any given run day.

VI. CONCLUSIONS AND RECOMMENDATIONS

During this test series, seven fuel additives (12% Rare Earth Hex-Cem, CV-100, Ferrocene, DGT-2, 12% Cerium Hex-Cem, XRG, and Cerium Octotate 12%) were evaluated to determine their effects on test cell exhaust opacity, on mean exhaust particle diameter, on exhaust particulate mass concentration, and on NO_x concentration. Principal results and recommendations are summarized as follow.

(a) Ferrocene, DGT-2, 12% Cerium Hex-Cem, and Cerium Octotate 12% reduced stack exhaust opacity from eleven to thirty-five percent. Of these four, DGT-2 and 12% Cerium Hex-Cem were the most effective. 12% Rare Earth Hex-Cem, CV-100, and XRG were ineffective at reducing stack opacity when mixed with JP-4 and burned in the NPS combustor.

(b) Particulate volume-to-surface mean particle diameter (d_{32}) varied from .13 to .28 microns throughout this investigation. An average value of .20 microns was observed, with a typical particle size variation of only .02 to .03 microns in any given test series. This range was considered an insignificant change in average particle diameter given the inaccuracies in measuring the individual transmittance values. It was concluded that the additives tested had no significant effect on d_{32}. Also, no significant changes in

mean particle diameter occurred between the engine and stack exhausts.

(c) Values of d_{32} listed in this report were obtained using a light transmittance technique. These optically measured values of d_{32} were compared to scanning electron microscope photographs of collected exhaust particulates. The range of particle sizes observed with the SEM consistently surrounded the optically obtained values, indicating the validity of the light transmission technique.

(d) The fuel additives which reduced stack opacity also reduced exhaust particulate mass concentration without reducing average particle diameter. Other investigators [Ref. 18] have found that manganese based additives can reduce particulate size without changing particulate mass. Barium additives have been found not to affect particulate size [Ref. 19]. This disparity of results may be due to the different types of additives and how they work, to the different combustor geometries (fuel atomization methods, residence times, quenching rates, etc.), and/or to the test conditions employed. Certainly there exists a need to evaluate various additives in one combustor design at various engine operating conditions.

(e) NO_x concentration at the test cell stack exhaust was not significantly changed by any of the fuel additives tested.

(f) Given the constraints of the testing apparatus employed in this investigation, it is felt that no further

worthwhile advances or conclusions can be made in this test series. It is recommended that the additives deemed effective at reducing opacity here, be further evaluated in a full size test cell employing an in service aircraft turbojet engine. It is further suggested that future tests avoid using a water cooled combustor. Instead a conventional hot-can combustor should be used exclusively to avoid the serious soot buildups experienced in this investigation.

TABLE I

ADDITIVES TESTED

1. 12% Rare Earth Hex-Cem (961 Control 12885)
   Mooney Chemicals, Inc.
   2301 Scranton Road
   Cleveland, Ohio 44113

2. CV-100; Universal Combustion Catalyst (Batch TH069/081280)
   Cavern Petrochemical Co., Ltd.
   Fort Erie, Ontario, Canada

3. Ferrocene Solution
   Arapaho Chemicals
   Boulder, Colorado

4. DGT-2 (Sample CSB-8-91)
   Apollo Technologies, Inc.
   One Apollo Drive
   Whippany, New Jersey 07981

5. 12% Cerium Hex-Cem (Control 380-2)
   Mooney Chemicals, Inc.
   2301 Scranton Road
   Cleveland, Ohio 44113

6. XRG; Fuel Synergist
   XRG International, Inc.
   4125 S.W. Martin Highway
   Stuart, Florida 33494

7. Cerium Octotate 12% in Mineral Spirits
   The Shepherd Chemical Company
   4900 Beech Street
   Cincinatti, Ohio 45212

TABLE II

TEST DATA AND RESULTS FOR 12% RARE EARTH HEX-CEM

Additive Concentration (ml./gal. JP-4)	$\dot{m}_{BP}$	$\dot{m}_p$	$\dot{m}_s$	$\dot{m}_e$	$\dot{m}_{e_T}$	$\dot{m}_f$	$\dot{m}_{aug.\ tube}$	Aug. Ratio
0.0	.754	.254	.176	.430	1.18	.019	6.71	4.67
10.05	.754	.254	.176	.430	1.18	.019	6.71	4.67
28.11	.729	.245	.196	.441	1.17	.021	6.75	4.77
0.0	.755	.249	.193	.442	1.20	.021	6.72	4.61

$\left(\frac{f}{a}\right)_p$	$\left(\frac{f}{a}\right)_{p+s}$	T_{BP}	T_c	T_R	T_{mix}	NO_x	Percent Opacity
.076	.045	569	1987	656	1084	1.70	41
.076	.045	569	1987	656	1084	1.75	41
.087	.048	569	1987	656	1103	1.85	42
.082	.046	569	1987	657	1091	1.72	42

Engine:

$T_\lambda(4500)$	$T_\lambda(6500)$	$T_\lambda(10140)$	d_{32}	C_{m_e}	$\dot{m}_{c_e}$
91.8	93.9	96.3	.18 ± .01	164	.15
89.3	92.0	95.1	.18 ± .01	219	.20
92.4	94.0	96.2	.21 ± .01	159	.15
90.3	93.0	95.7	.17 ± .01	192	.18

Stack:

$T_\lambda(4500)$	$T_\lambda(6500)$	$T_\lambda(10140)$	d_{32}	C_{m_s}	$\dot{m}_{c_s}$	$\frac{\dot{m}_{c_e}}{\dot{m}_{c_s}}$
77.2	83.1	89.3	.18 ± .01	32	.10	1.5
70.2	78.0	86.6	.16 ± .01	43	.13	1.5
72.3	78.6	85.7	.21 ± .01	41	.13	1.1
70.7	78.2	86.2	.17 ± .01	43	.13	1.3

See table of symbols and abbreviations for explanation of column headings/units.

TABLE III

TEST DATA AND RESULTS FOR CV-100

Additive Concentration (ml./gal. JP-4)	$\dot{m}_{BP}$	$\dot{m}_p$	$\dot{m}_s$	$\dot{m}_e$	$\dot{m}_{e_T}$	$\dot{m}_f$	$\dot{m}_{aug.\ tube}$	Aug. Ratio
0.0	.827	.267	.210	.477	1.30	.018	6.85	4.25
2.36	.771	.262	.222	.484	1.26	.018	7.10	4.66
32.56	.771	.262	.222	.484	1.26	.018	7.10	4.66
0.0	.771	.262	.222	.484	1.26	.018	7.10	4.66

$\left(\frac{f}{a}\right)_p$	$\left(\frac{f}{a}\right)_{p+s}$	T_{BP}	T_c	T_R	T_{mix}	NO_x	Percent Opacity
.069	.039	561	2007	648	1090	1.35	33
.070	.038	561	2000	641	1116	1.35	34
.070	.038	561	2000	641	1116	1.50	37
.070	.038	561	2000	641	1116	1.45	40

Engine:

$T_\lambda(4500)$	$T_\lambda(6500)$	$T_\lambda(10140)$	d_{32}	C_{m_e}	$\dot{m}_{c_e}$
92.9	94.6	96.6	.20 ± .01	143	.15
93.5	94.8	96.5	.24 ± .01	147	.15
92.9	94.4	96.3	.23 ± .01	157	.16
91.2	93.1	95.6	.21 ± .01	184	.18

Stack:

$T_\lambda(4500)$	$T_\lambda(6500)$	$T_\lambda(10140)$	d_{32}	C_{m_s}	$\dot{m}_{c_s}$	$\frac{\dot{m}_{c_e}}{\dot{m}_{c_s}}$
80.0	85.3	90.8	.18 ± .01	28	.09	1.7
81.0	86.0	91.5	.17 ± .01	25	.08	1.8
73.9	81.1	88.5	.15 ± .01	35	.12	1.4
76.2	81.2	87.7	.21 ± .01	35	.11	1.6

See table of symbols and abbreviations for explanation of column headings/units.

TABLE IV

TEST DATA AND RESULTS FOR FERROCENE

Additive Concentration (ml./gal. JP-4)	$\dot{m}_{BP}$	$\dot{m}_p$	$\dot{m}_s$	$\dot{m}_e$	$\dot{m}_{e_T}$	$\dot{m}_f$	$\dot{m}_{aug.\ tube}$	Aug. Ratio
0.0	.845	.248	.183	.431	1.28	.019	6.91	4.41
28.48	.845	.248	.183	.431	1.28	.019	6.91	4.41
0.0	.845	.248	.183	.431	1.28	.019	6.91	4.41
28.48	.845	.248	.183	.431	1.28	.019	6.91	4.41

$\left(\frac{f}{a}\right)_p$	$\left(\frac{f}{a}\right)_{p+s}$	T_{BP}	T_c	T_R	T_{mix}	NO_x	Percent Opacity
.078	.045	562	1994	652	1045	1.60	42
.078	.045	562	1994	652	1045	1.52	32
.078	.045	562	1968	652	1037	1.95	63
.078	.045	562	1968	652	1037	2.10	55

Engine:

$T_\lambda(4500)$	$T_\lambda(6500)$	$T_\lambda(10140)$	d_{32}	C_{m_e}	$\dot{m}_{c_e}$
87.8	90.9	94.3	.19 ± .01	246	.23
91.7	94.1	96.5	.16 ± .01	161	.15
79.5	83.7	88.9	.23 ± .01	490	.46
81.7	85.1	90.1	.23 ± .01	434	.41

Stack:

$T_\lambda(4500)$	$T_\lambda(6500)$	$T_\lambda(10140)$	d_{32}	C_{m_s}	$\dot{m}_{c_s}$	$\frac{\dot{m}_{c_e}}{\dot{m}_{c_s}}$
70.2	76.3	84.4	.21 ± .01	45	.15	1.6
84.2	87.1	91.4	.24 ± .01	24	.08	2.0
52.1	57.9	68.6	.28 ± .01	99	.32	1.5
56.4	62.6	72.1	.27 ± .01	87	.28	1.5

See table of symbols and abbreviations for explanation of column headings/units.

TABLE V

TEST DATA AND RESULTS FOR DGT-2

Additive Concentration (ml./gal. JP-4)	$\dot{m}_{BP}$	$\dot{m}_p$	$\dot{m}_s$	$\dot{m}_e$	$\dot{m}_{e_T}$	$\dot{m}_f$	$\dot{m}_{aug.\ tube}$	Aug. Ratio
0.0	.768	.245	.181	.426	1.19	.019	6.74	4.64
27.35	.793	.259	.176	.435	1.23	.020	6.91	4.63
0.0	.779	.244	.193	.437	1.22	.020	7.00	4.76

$\left(\frac{f}{a}\right)_p$	$\left(\frac{f}{a}\right)_{p+s}$	T_{BP}	T_c	T_R	T_{mix}	NO_x	Percent Opacity
.078	.045	560	1983	642	1067	1.46	41
.078	046	561	1983	643	1064	1.50	31
.083	.046	560	1983	647	1071	1.51	44

Engine:

$T_\lambda(4500)$	$T_\lambda(6500)$	$T_\lambda(10140)$	d_{32}	C_{m_e}	$\dot{m}_{c_e}$
93.2	95.1	97.1	.15 ± .01	130	.12
94.7	96.2	97.8	.15 ± .01	99	.10
90.2	92.7	95.6	.17 ± .01	192	.18

Stack:

$T_\lambda(4500)$	$T_\lambda(6500)$	$T_\lambda(10140)$	d_{32}	C_{m_s}	$\dot{m}_{c_s}$	$\frac{\dot{m}_{c_e}}{\dot{m}_{c_s}}$
78.7	86.0	92.1	.10 ± .01	28	.09	1.4
80.6	86.4	92.1	.13 ± .01	28	.09	1.1
70.0	76.5	84.9	.19 ± .01	45	.15	1.2

See table of symbols and abbreviations for explanation of column headings/units.

TABLE VI

TEST DATA AND RESULTS FOR 12% CERIUM HEX-CEM

Additive Concentration (ml./gal. JP-4)	$\dot{m}_{BP}$	$\dot{m}_p$	$\dot{m}_s$	$\dot{m}_e$	$\dot{m}_{e_T}$	$\dot{m}_f$	$\dot{m}_{aug.\ tube}$	Aug. Ratio
0.0	.772	.267	.177	.444	1.22	.018	6.80	4.59
31.90	.772	.267	.177	.444	1.22	.018	6.80	4.59
30.54	.797	.274	.220	.494	1.29	.019	6.84	4.30
0.0	.797	.274	.220	.494	1.29	.019	6.84	4.30

$\left(\frac{f}{a}\right)_p$	$\left(\frac{f}{a}\right)_{p+s}$	T_{BP}	T_c	T_R	T_{mix}	NO_x	Percent Opacity
.067	.041	556	1966	646	1071	1.50	43
.067	.041	556	1966	646	1071	1.58	34
.069	.038	556	1981	647	1101	2.10	31
.069	.038	556	1981	647	1101	2.20	48

Engine:

$T_\lambda(4500)$	$T_\lambda(6500)$	$T_\lambda(10140)$	d_{32}	C_{m_e}	$\dot{m}_{c_e}$
86.5	89.9	93.7	.18 ± .01	283	.26
90.0	92.3	95.1	.21 ± .01	206	.19
91.1	93.0	95.4	.22 ± .01	193	.20
85.4	89.0	93.0	.19 ± .01	304	.31

Stack:

$T_\lambda(4500)$	$T_\lambda(6500)$	$T_\lambda(10140)$	d_{32}	C_{m_s}	$\dot{m}_{c_s}$	$\frac{\dot{m}_{c_e}}{\dot{m}_{c_s}}$
72.3	79.7	87.5	.16 ± .01	40	.12	2.1
78.7	84.5	90.6	.16 ± .01	29	.09	2.1
75.5	81.4	88.3	.18 ± .01	35	.11	1.7
61.2	71.2	81.3	.17 ± .01	59	.19	1.7

See table of symbols and abbreviations for explanation of column headings/units.

TABLE VII

TEST DATA AND RESULTS FOR XRG

Additive Concentration (ml./gal. JP-4)	$\dot{m}_{BP}$	$\dot{m}_p$	$\dot{m}_s$	$\dot{m}_e$	$\dot{m}_{e_T}$	$\dot{m}_f$	$\dot{m}_{aug.\ tube}$	Aug. Ratio
28.24	.803	.256	.211	.467	1.27	.019	6.84	4.39
0.0	.803	.256	.211	.467	1.27	.019	6.84	4.39

$\left(\frac{f}{a}\right)_p$	$\left(\frac{f}{a}\right)_{p+s}$	T_{BP}	T_c	T_R	T_{mix}	NO_x	Percent Opacity
.073	.040	556	1993	644	1084	1.90	39
.073	.040	556	1993	644	1084	2.10	38

Engine:

$T_\lambda(4500)$	$T_\lambda(6500)$	$T_\lambda(10140)$	d_{32}	C_{m_e}	$\dot{m}_{ce}$
87.7	90.5	93.8	.21 ± .01	262	.26
87.7	90.5	93.8	.21 ± .01	262	.26

Stack:

$T_\lambda(4500)$	$T_\lambda(6500)$	$T_\lambda(10140)$	d_{32}	C_{m_s}	$\dot{m}_{c_s}$	$\frac{\dot{m}_{c_e}}{\dot{m}_{c_s}}$
70.6	78.4	86.7	.16 ± .01	42	.13	1.9
70.2	77.6	85.9	.17 ± .01	44	.14	1.9

See table of symbols and abbreviations for explanation of column headings/units.

TABLE VIII

TEST DATA AND RESULTS FOR CERIUM OCTOTATE 12%

Additive Concentration (ml./gal. JP-4)	$\dot{m}_{BP}$	$\dot{m}_p$	$\dot{m}_s$	$\dot{m}_e$	$\dot{m}_{eT}$	$\dot{m}_f$	$\dot{m}_{aug.\ tube}$	Aug. Ratio
22.02	.720	.267	.207	.474	1.19	.018	6.63	4.55
0.0	.720	.267	.207	.474	1.19	.018	6.63	4.55
22.02	.720	.267	.207	.474	1.19	.018	6.63	4.55
0.0	.720	.267	.207	.474	1.19	.018	6.63	4.55

$\left(\frac{f}{a}\right)_p$	$\left(\frac{f}{a}\right)_{p+s}$	T_{BP}	T_c	T_R	T_{mix}	NO_x	Percent Opacity
.068	.038	556	2006	655	1132	---	29
.068	.038	556	2006	655	1132	---	36
.068	.038	556	1981	655	1122	---	34
.068	.038	556	1981	655	1122	---	38

Engine:

$T_\lambda(4500)$	$T_\lambda(6500)$	$T_\lambda(10140)$	d_{32}	C_{m_e}	$\dot{m}_{c_e}$
92.7	94.8	97.0	.15 ± .01	135	.13
88.7	91.9	95.2	.16 ± .01	223	.22
91.4	93.9	96.4	.16 ± .01	166	.16
89.1	92.2	95.4	.16 ± .01	213	.20

Stack:

$T_\lambda(4500)$	$T_\lambda(6500)$	$T_\lambda(10140)$	d_{32}	C_{m_s}	$\dot{m}_{c_s}$	$\frac{\dot{m}_{c_e}}{\dot{m}_{c_s}}$
80.8	86.0	91.4	.16 ± .01	27	.08	1.6
74.7	81.3	88.5	.16 ± .01	36	.11	1.9
77.3	83.1	89.7	.17 ± .01	31	.10	1.7
74.7	81.3	88.5	.16 ± .01	36	.11	1.8

See table of symbols and abbreviations for explanation of column headings/units.

TABLE IX

ENGINE EXHAUST MEAN PARTICLE DIAMETERS VS SEM
MEASURED EXHAUST PARTICLE SIZES

Additive Concentration (ml./gal. JP-4)	d_{32} Measured Optically	Particulate Sizes from SEM
12% Rare Earth Hex-Cem (0.0)	.18 ± .01	.05 to .25
12% Rare Earth Hex-Cem (10.05)	.18 ± .01	.08 to .28
12% Rare Earth Hex-Cem (28.11)	.21 ± .01	.05 to .23
12% Rare Earth Hex-Cem (0.0)	.17 ± .01	.08 to .25
CV-100 (0.0)	.20 ± .01	.05 to .25
CV-100 (2.36)	.24 ± .01	.08 to .30
CV-100 (32.56)	.23 ± .01	.10 to .28
CV-100 (0.0)	.21 ± .01	.08 to .30
Ferrocene (28.48)	.16 ± .01	.05 to .23
Ferrocene (0.0)	.23 ± .01	.05 to .25
DGT-2 (0.0)	.15 ± .01	.05 to .18
DGT-2 (27.35)	.15 ± .01	.05 to .18
DGT-2 (0.0)	.17 ± .01	.05 to .20
12% Cerium Hex-Cem (0.0)	.18 ± .01	.08 to .20
12% Cerium Hex-Cem (31.90)	.21 ± .01	.08 to .25
12% Cerium Hex-Cem (30.54)	.22 ± .01	.05 to .20
12% Cerium Hex-Cem (0.0)	.19 ± .01	.05 to .18
XRG (28.24)	.21 ± .01	.05 to .20
XRG (0.0)	.21 ± .01	.08 to .20

Cerium Octotate (No SEM photos available)

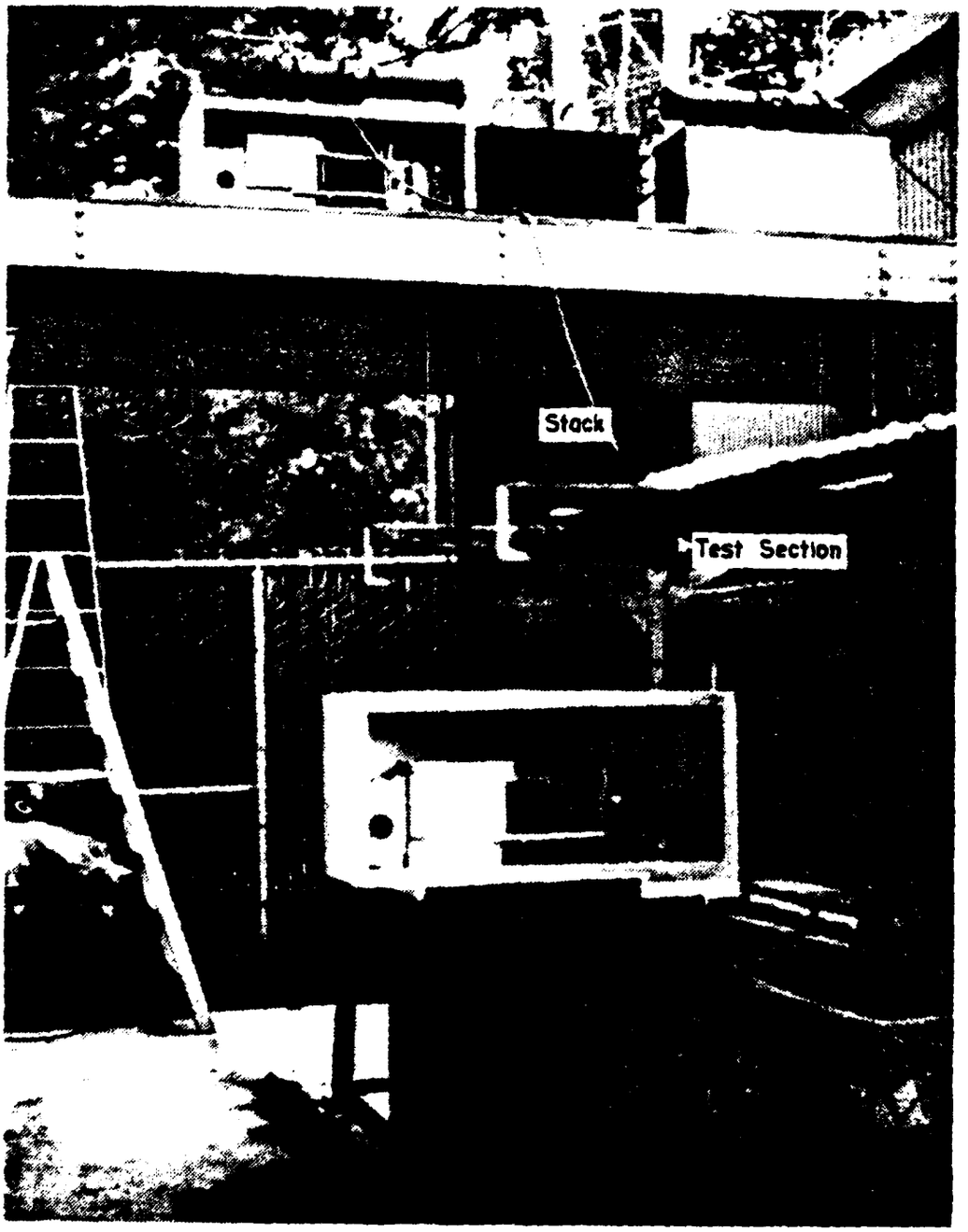

Figure 1. Sub-Scale Turbojet Test Cell
(Figure 2 of Reference 12)

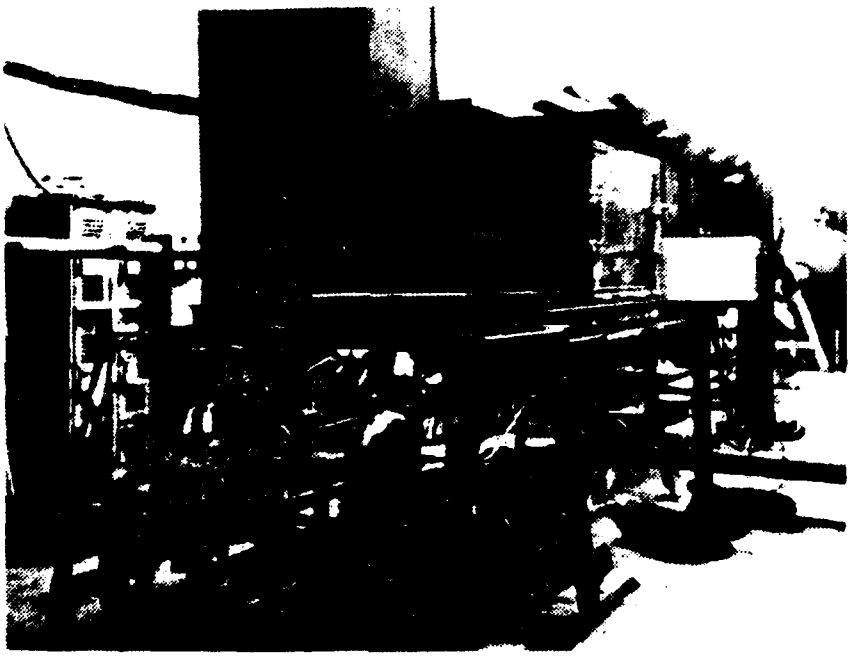

Figure 2

Photograph of Sub-Scale Test Cell
(Figure 3 of Reference 12)

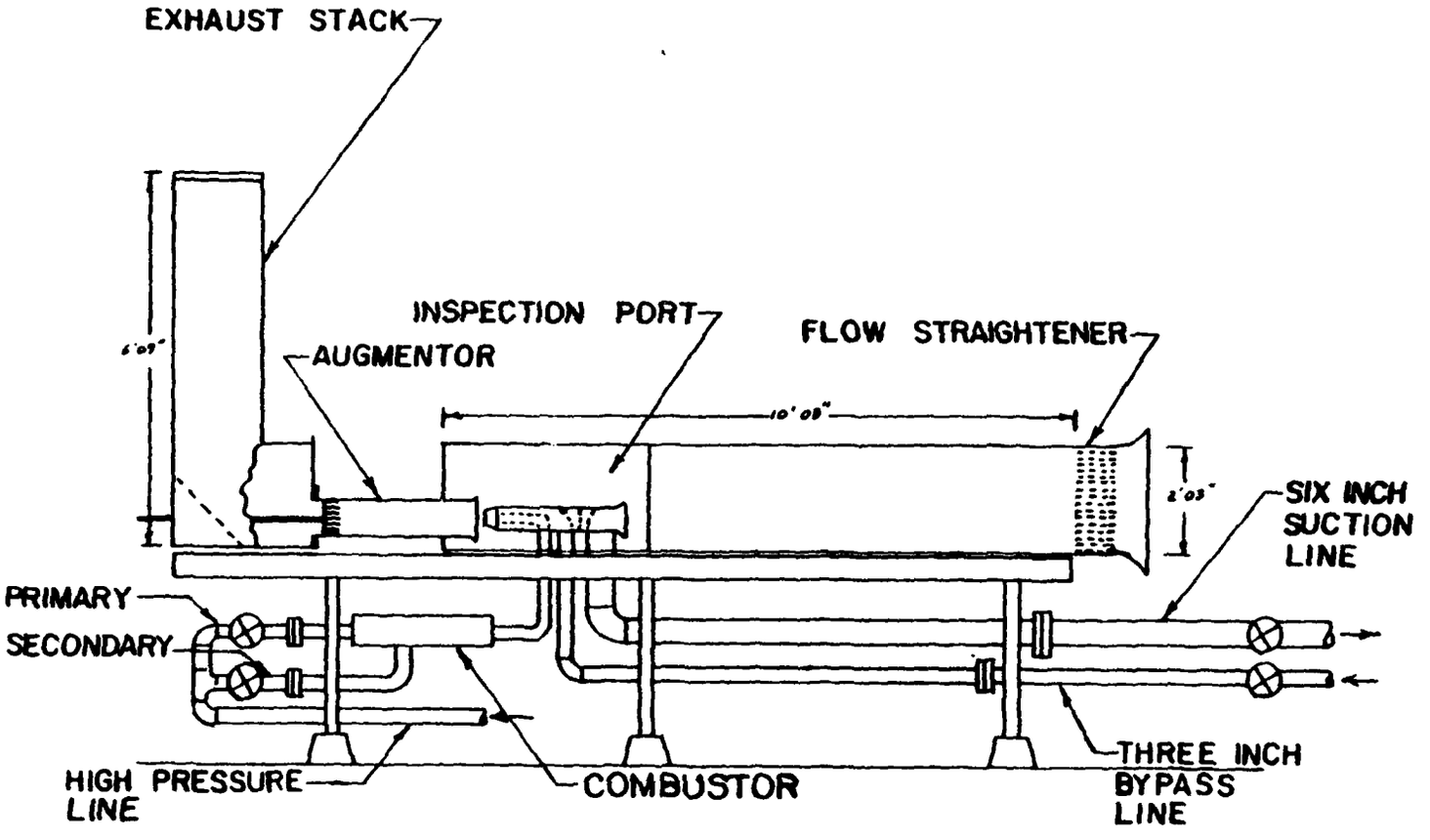

Figure 3. Sub-Scale Test Cell Plumbing
(Figure 4 of Reference 12)

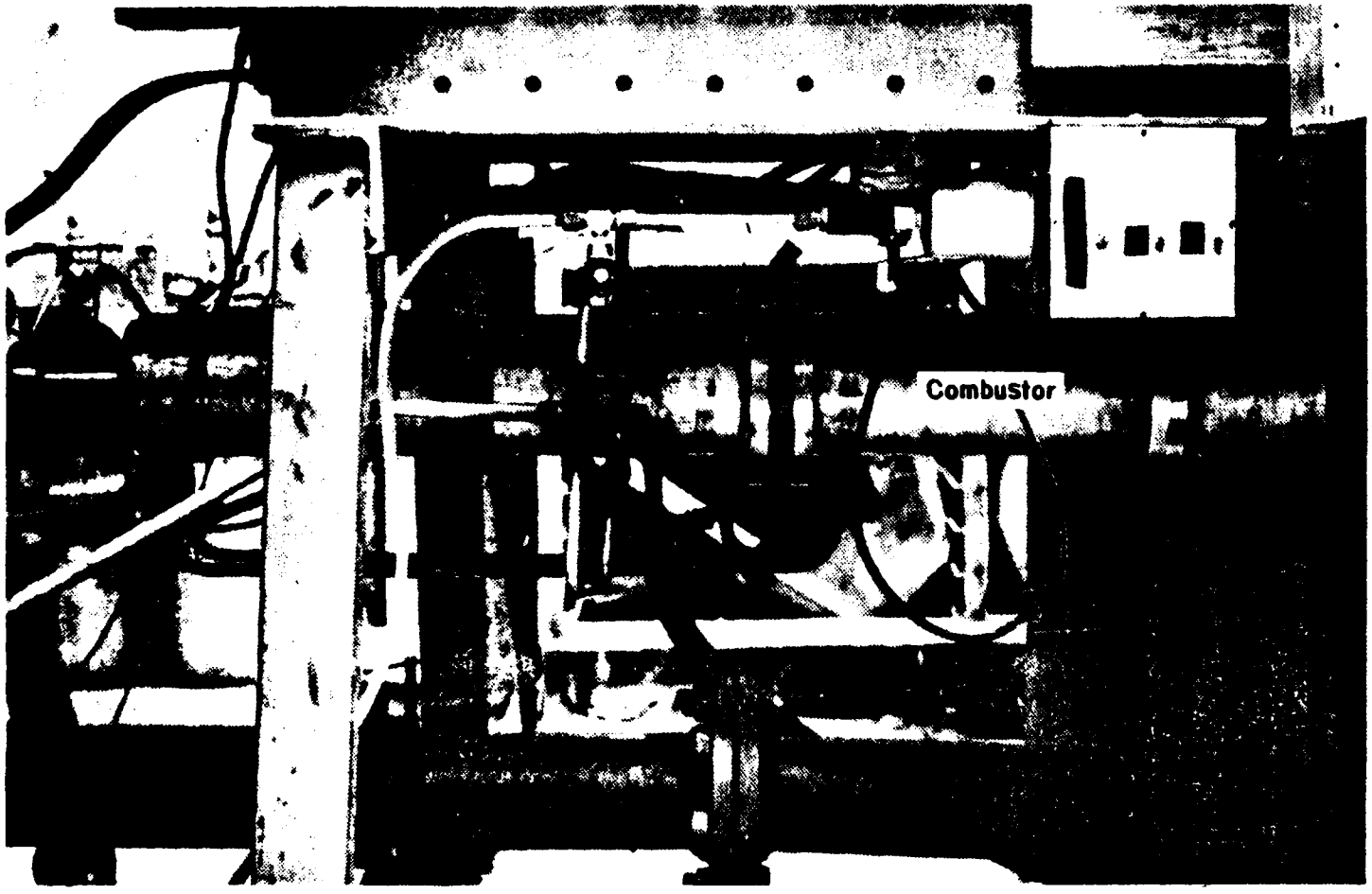

Figure 4. Sub-Scale Turbojet Test Cell Combustor
(Figure 5 of Reference 12)

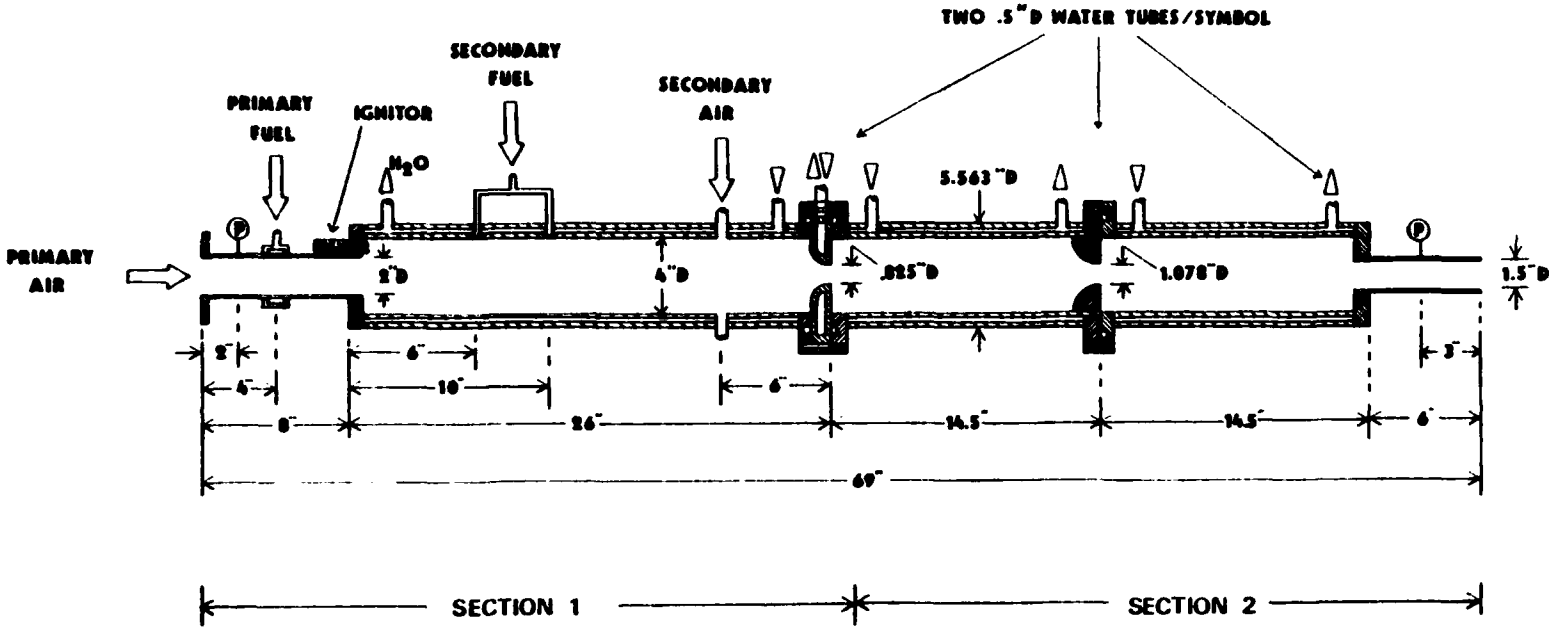

Figure 5. Schematic of Water-Cooled Ramjet Type Dump-Combustor
(Figure 3 of Reference 3)

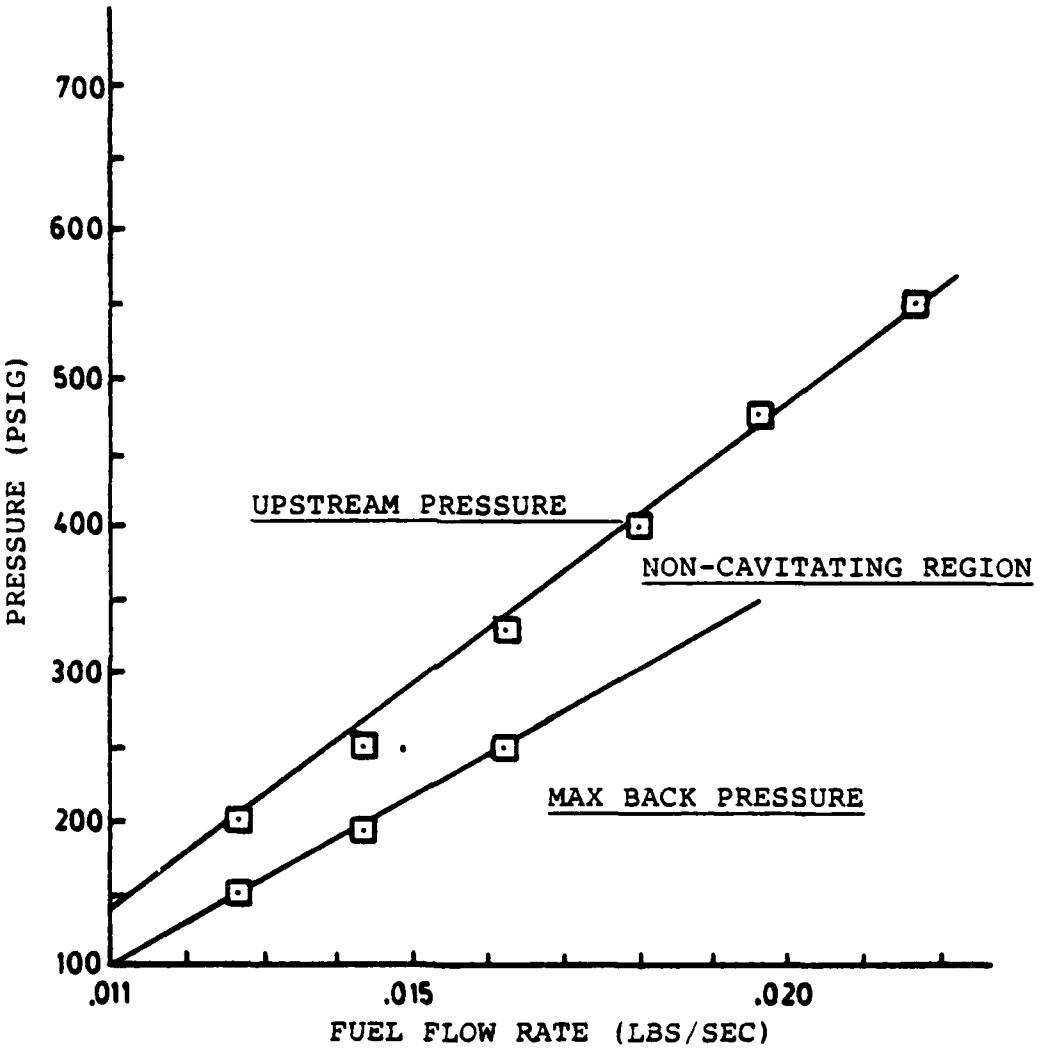

Figure 6. Cavitating Venturi Pressure vs JP-4 Fuel Flow Rate for .017-Inch Diameter Venturi

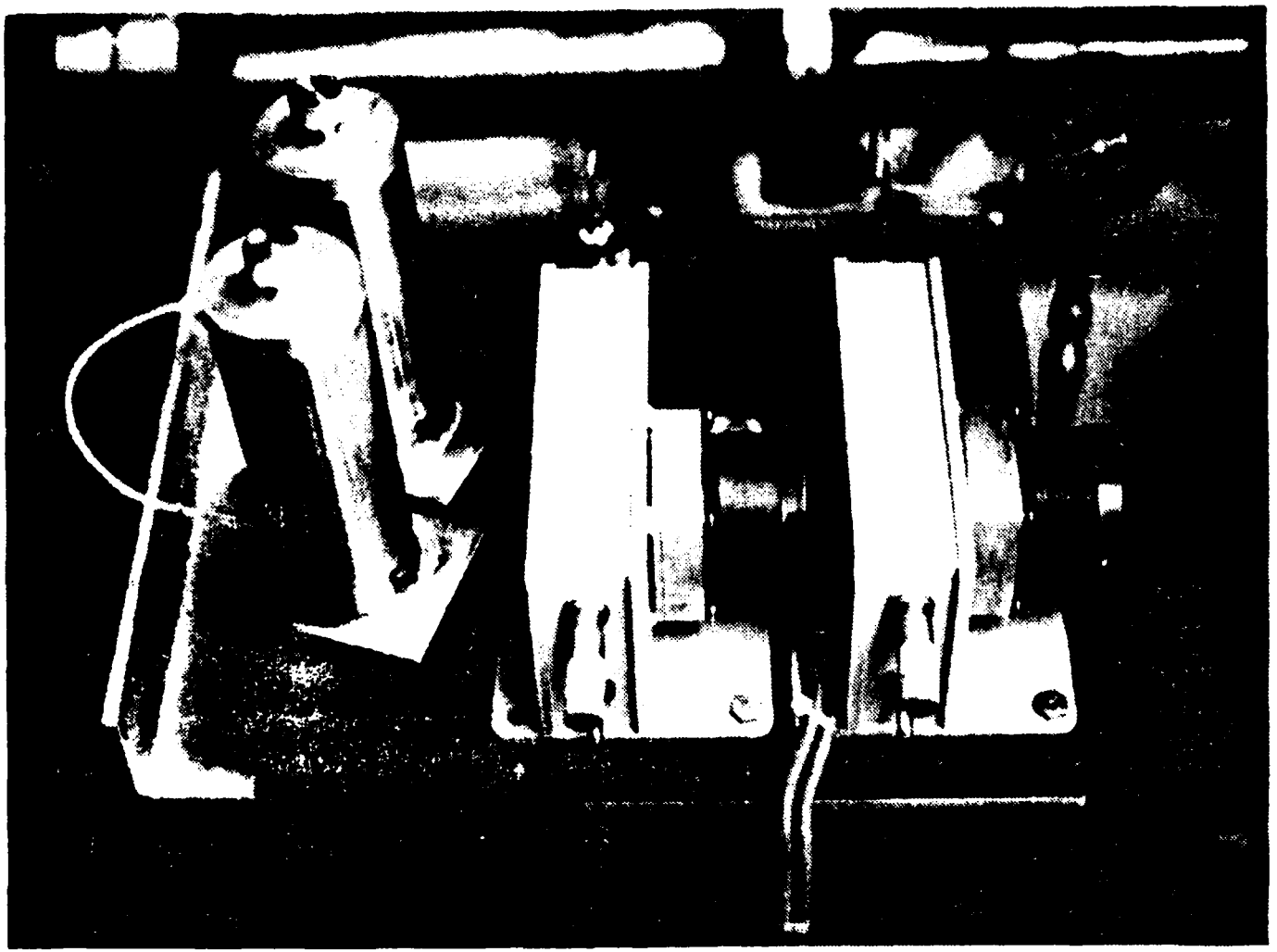

Figure 7. Precision Metering Pumps
(Figure 10 of Reference 12)

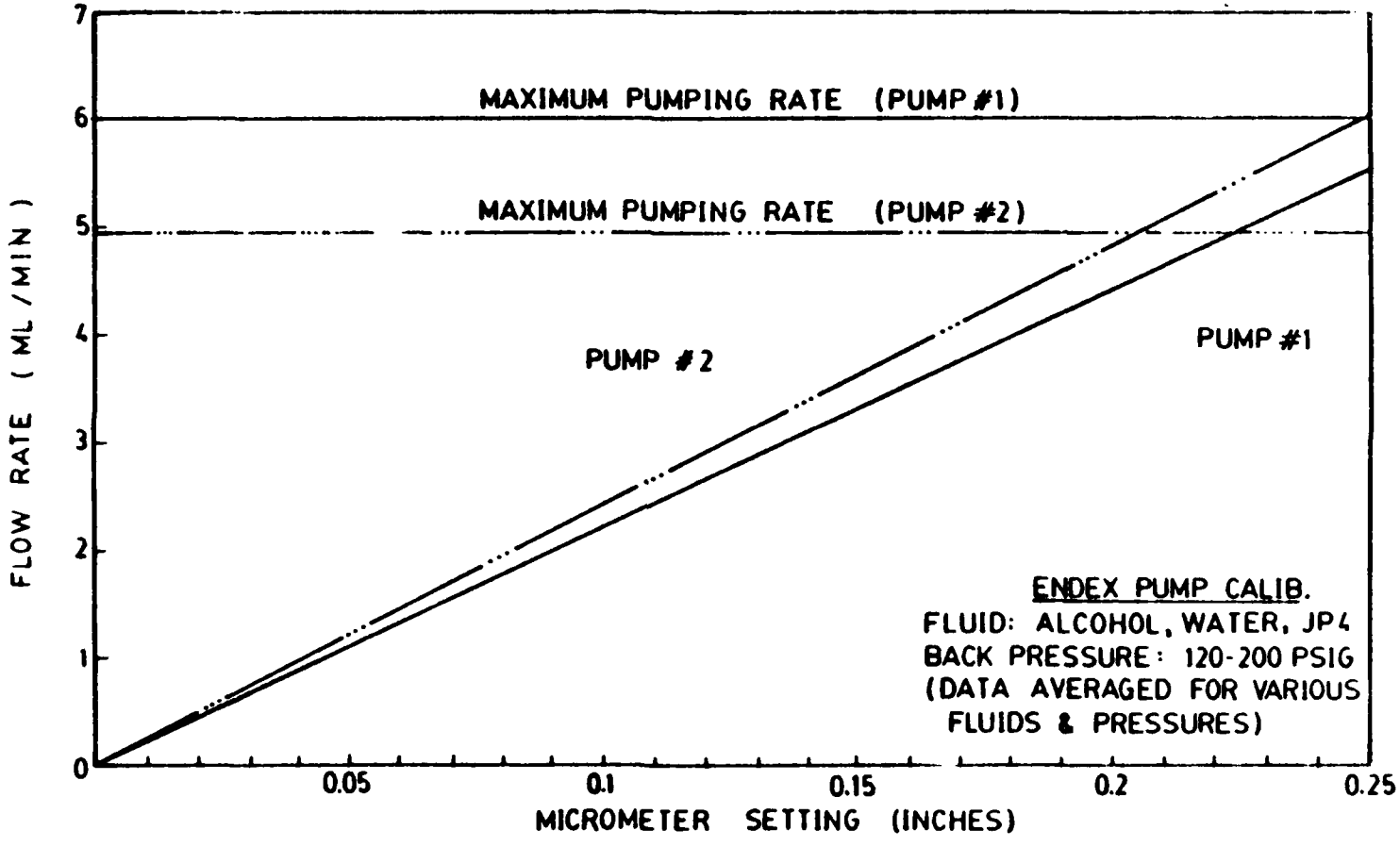

Figure 8. Precision Metering Pumps Calibration Curves

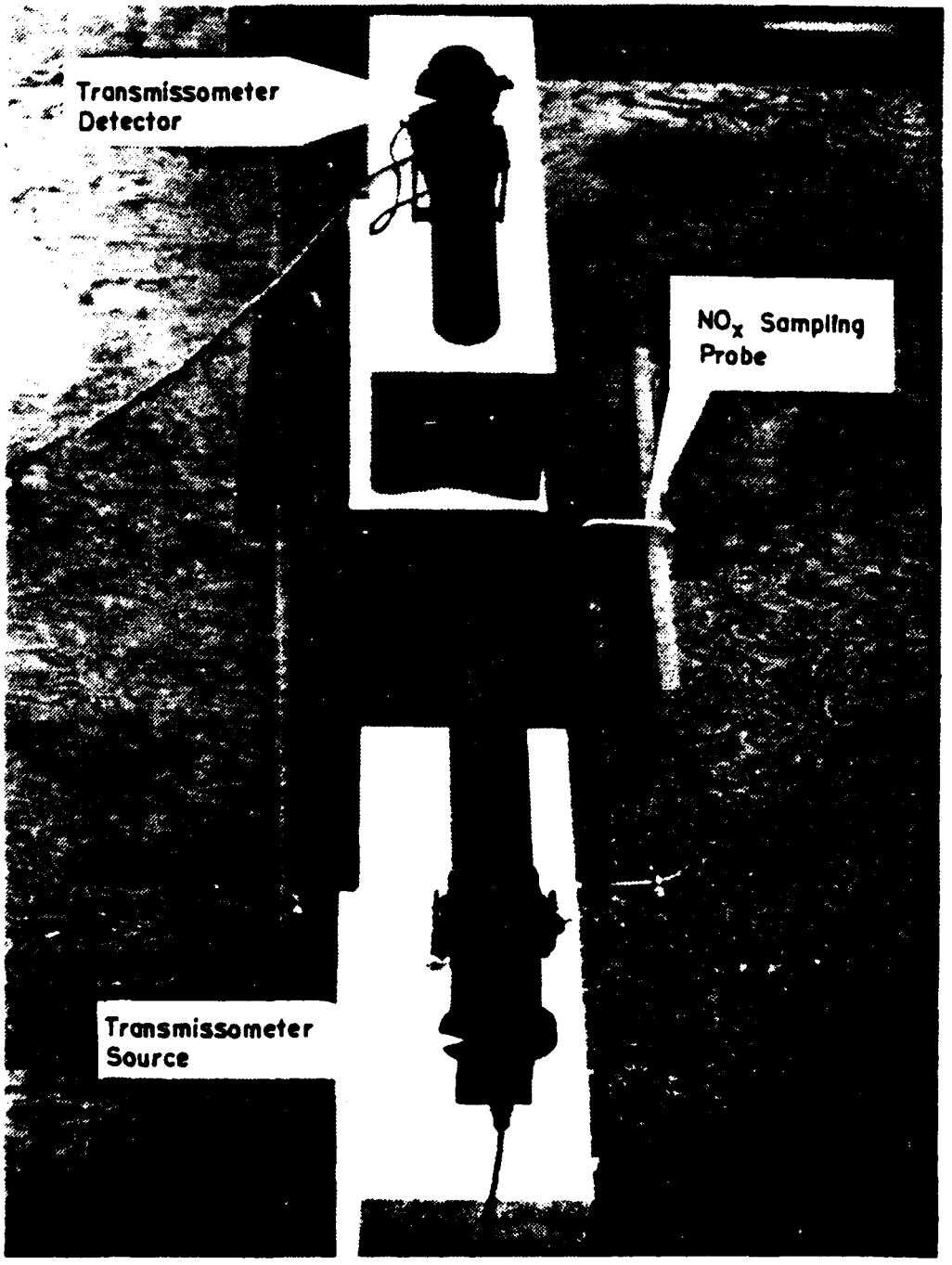

Figure 9. Transmissometer Source/Detector Unit
(Figure 13 of Reference 12)

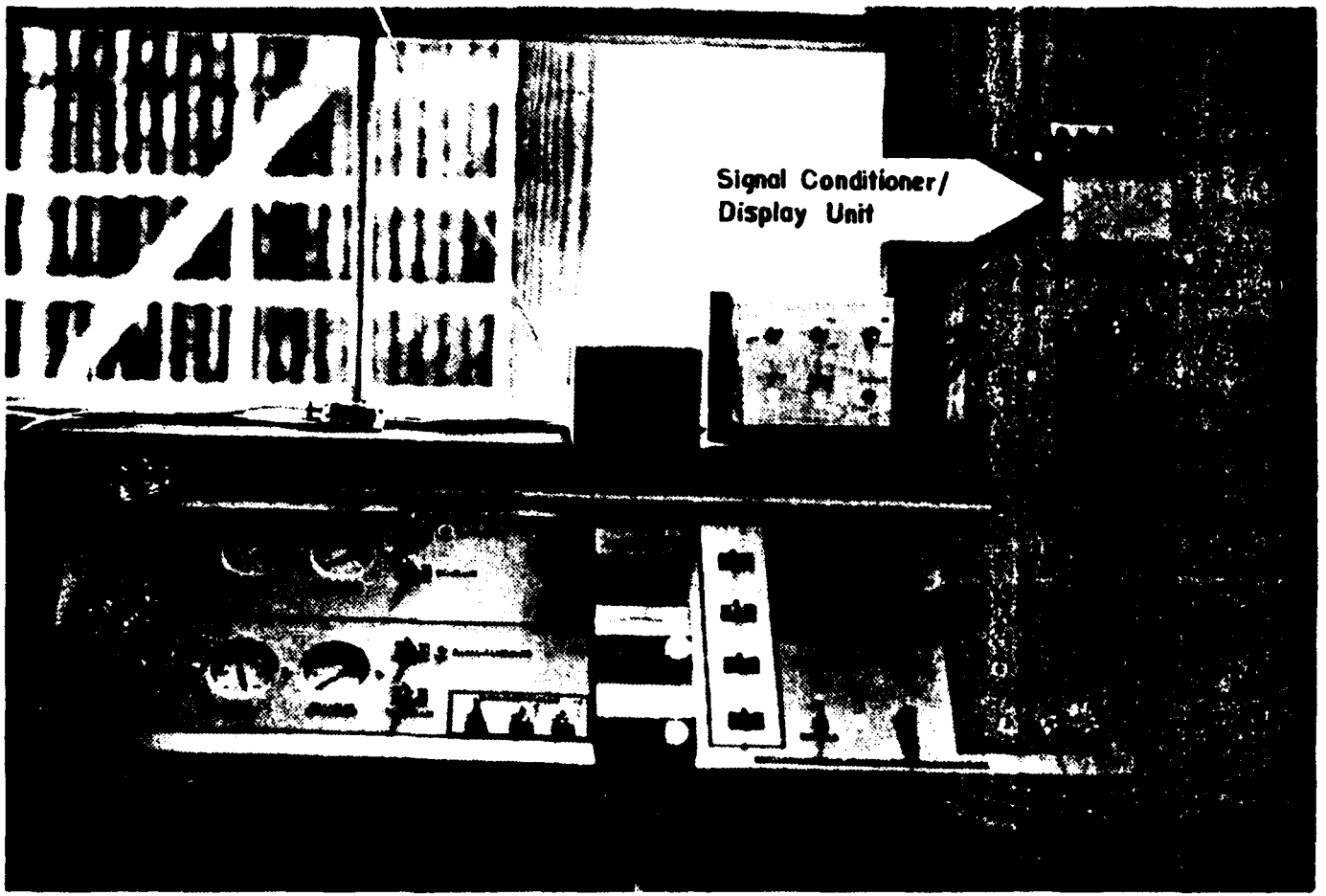

Figure 10. Remote Control Panel and Signal Conditioner/Display Unit
(Figure 8 of Reference 12)

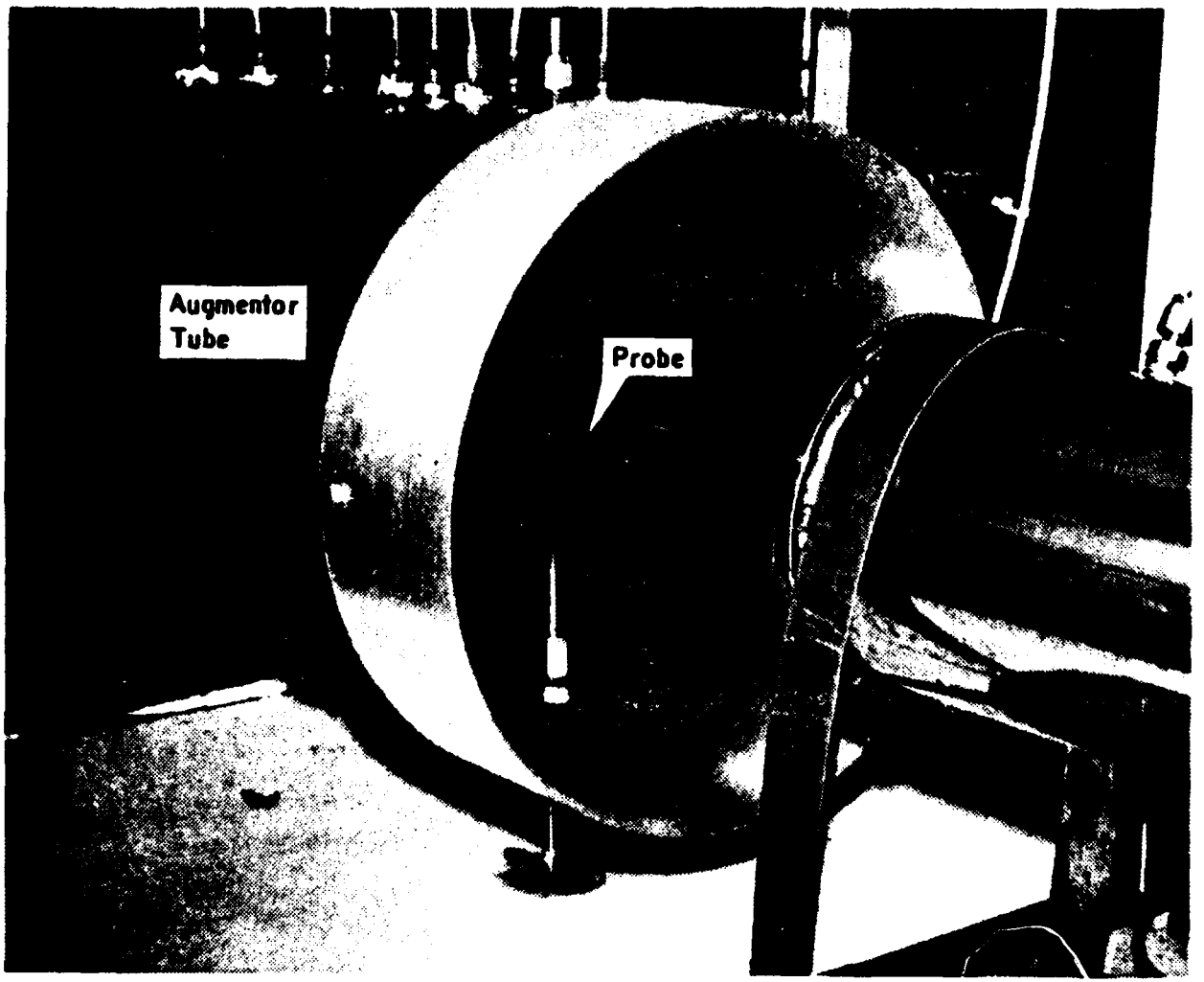

Figure 11. Sampling Probe
(Figure 19 of Reference 12)

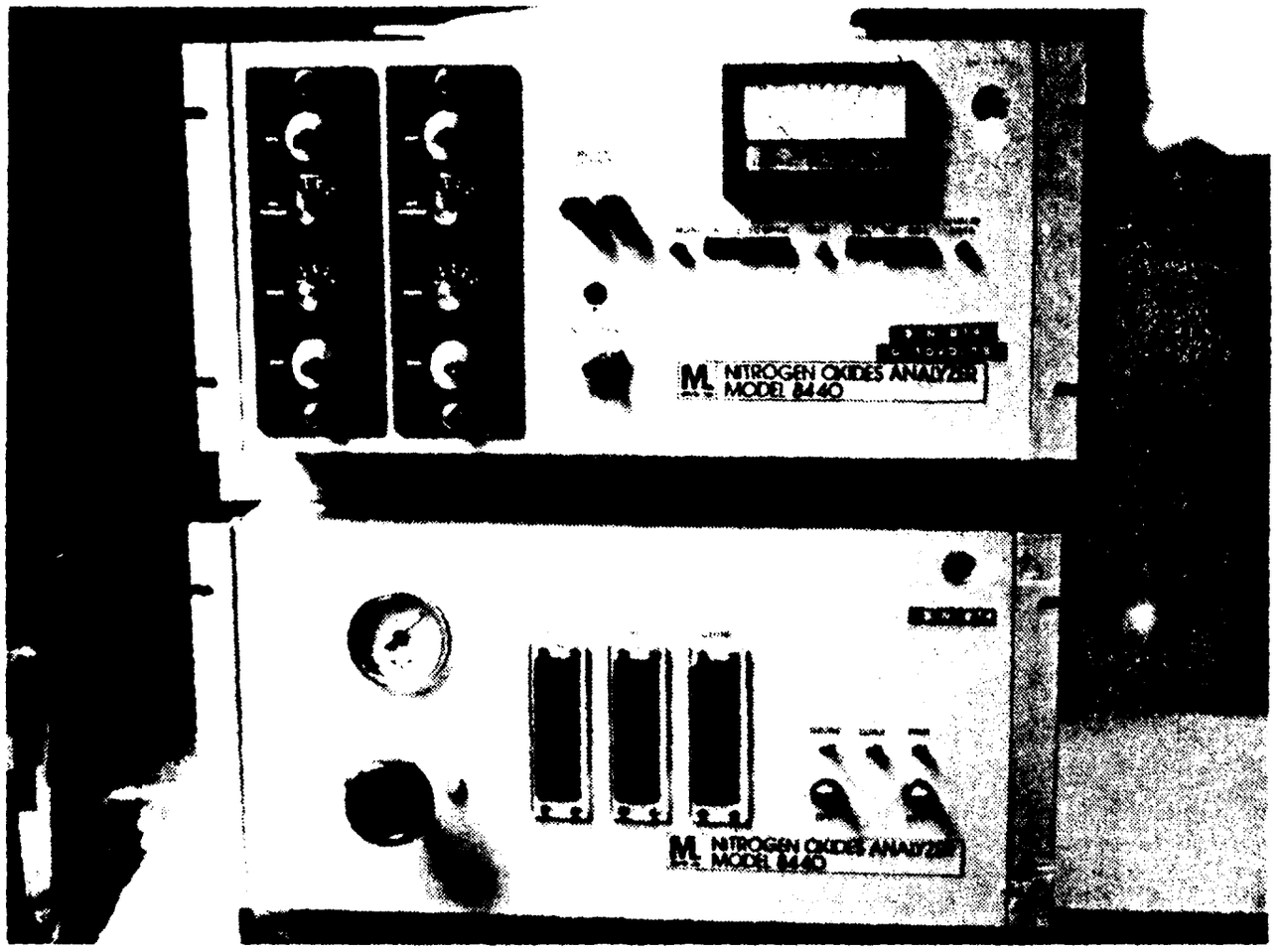

Figure 12. Nitrogen Oxides Analyzer
(Figure 20 of Reference 12)

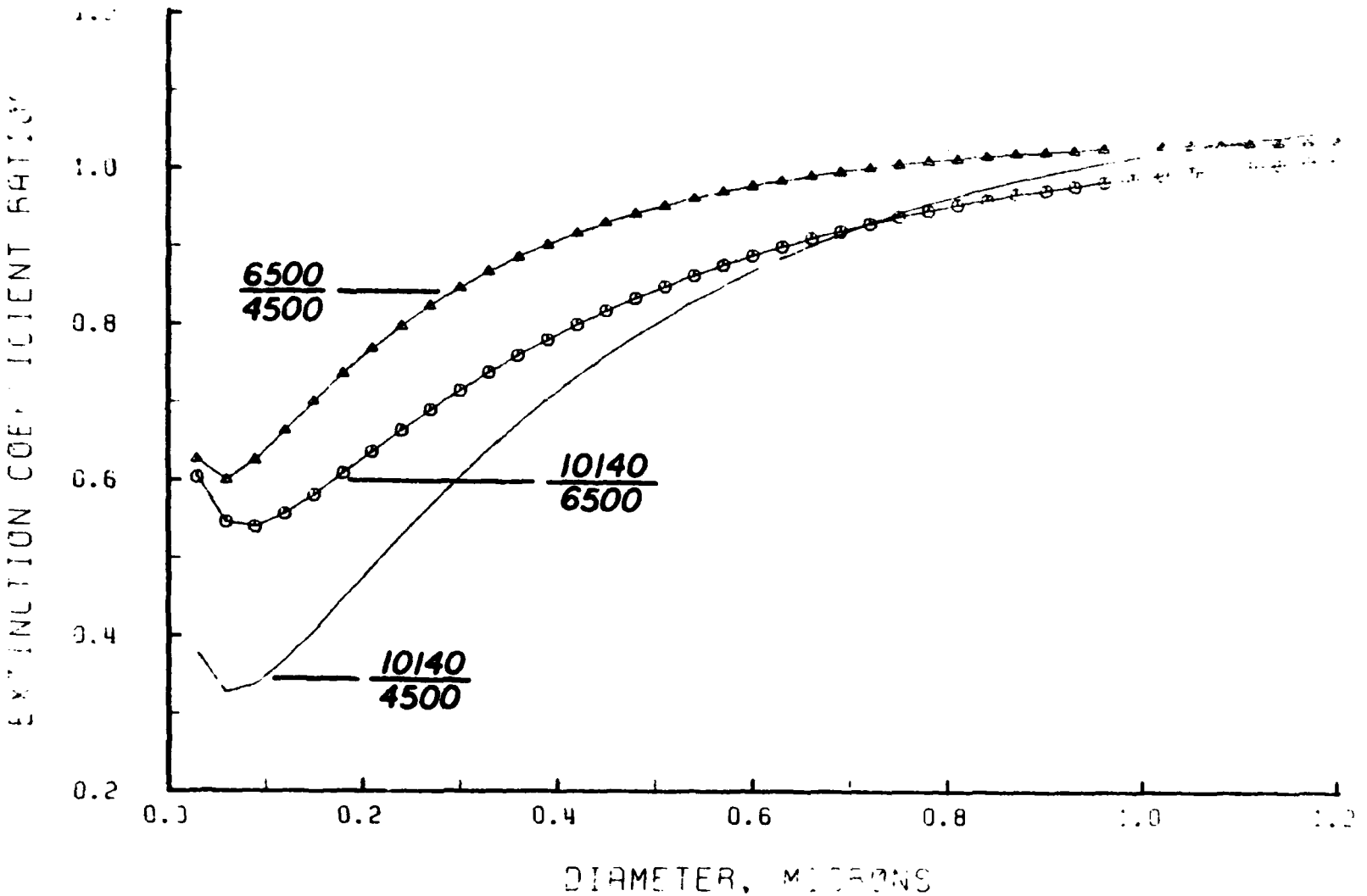

Figure 13. d_{32} vs Extinction Coefficient Ratios (λ = 4500 Å, λ = 6500 Å, λ = 10140 Å), for m = 1.95 - .66i, σ = 2.0

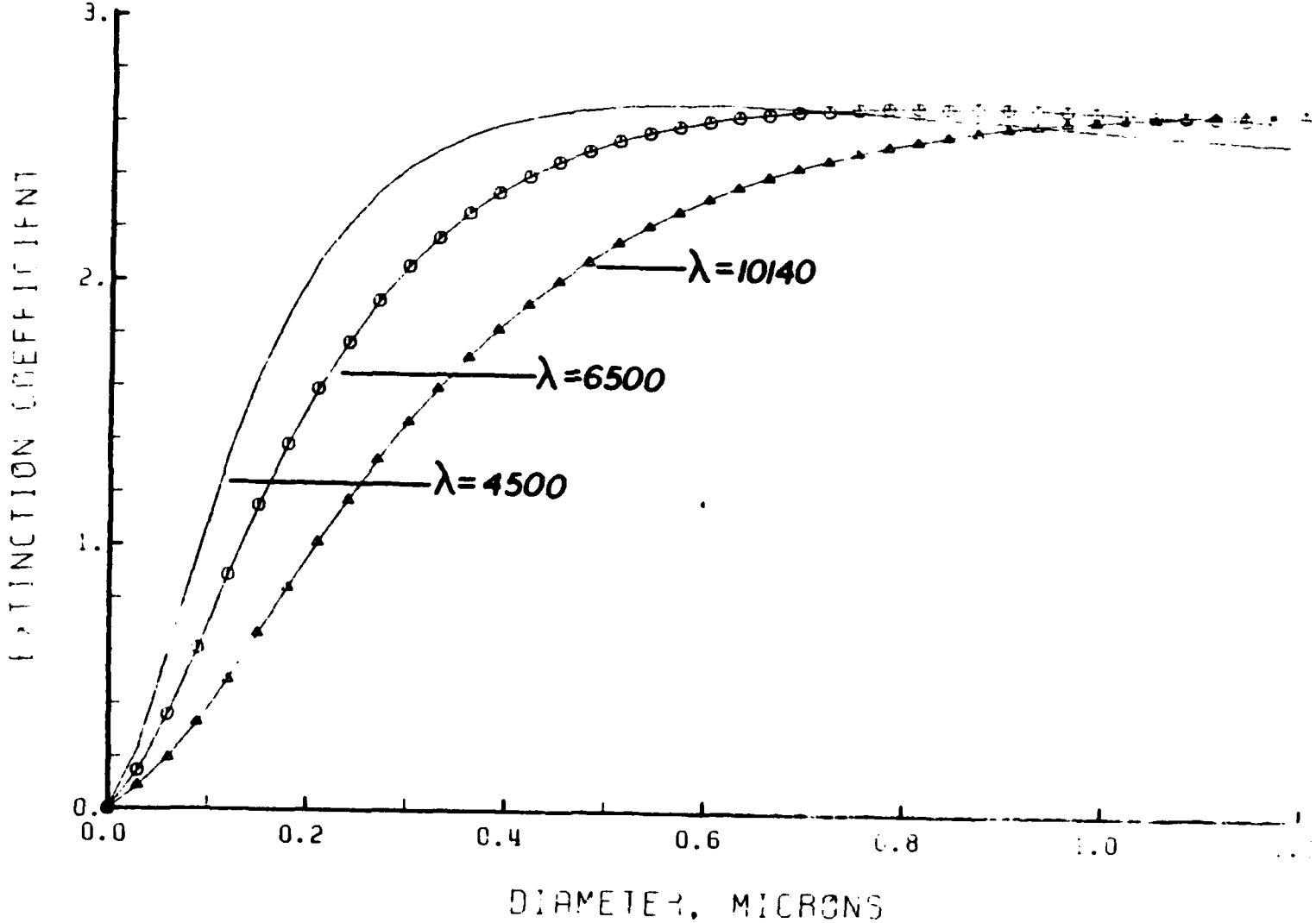

Figure 14. d_{32} vs Extinction Coefficient (λ = 4500 Å, λ = 6500 Å, λ = 10140 Å), for m = 1.95 - .66i, σ = 2.0

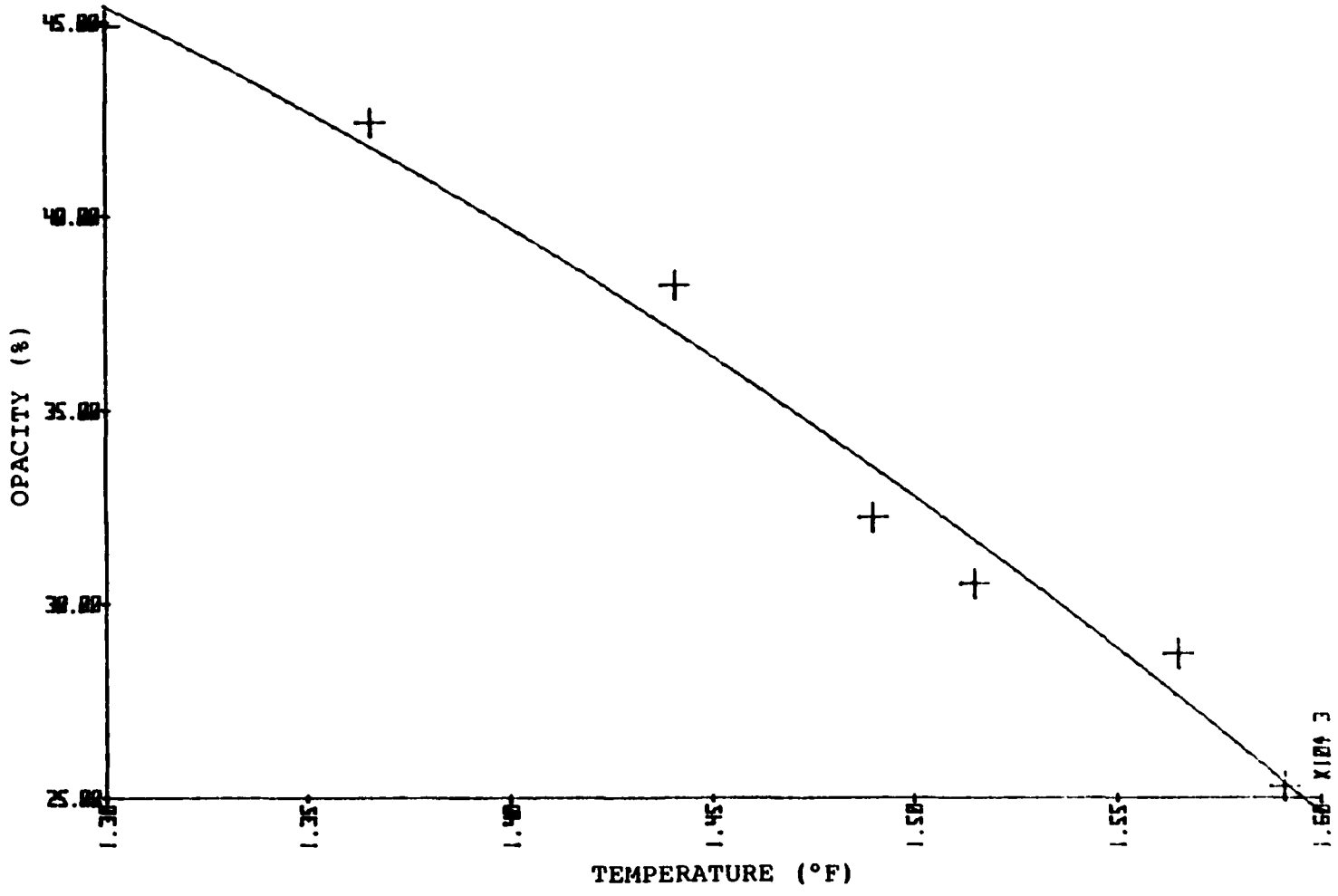

Figure 15. Combustor Exhaust Temperature (T_c) vs Test Cell Stack Exhaust Gas Opacity

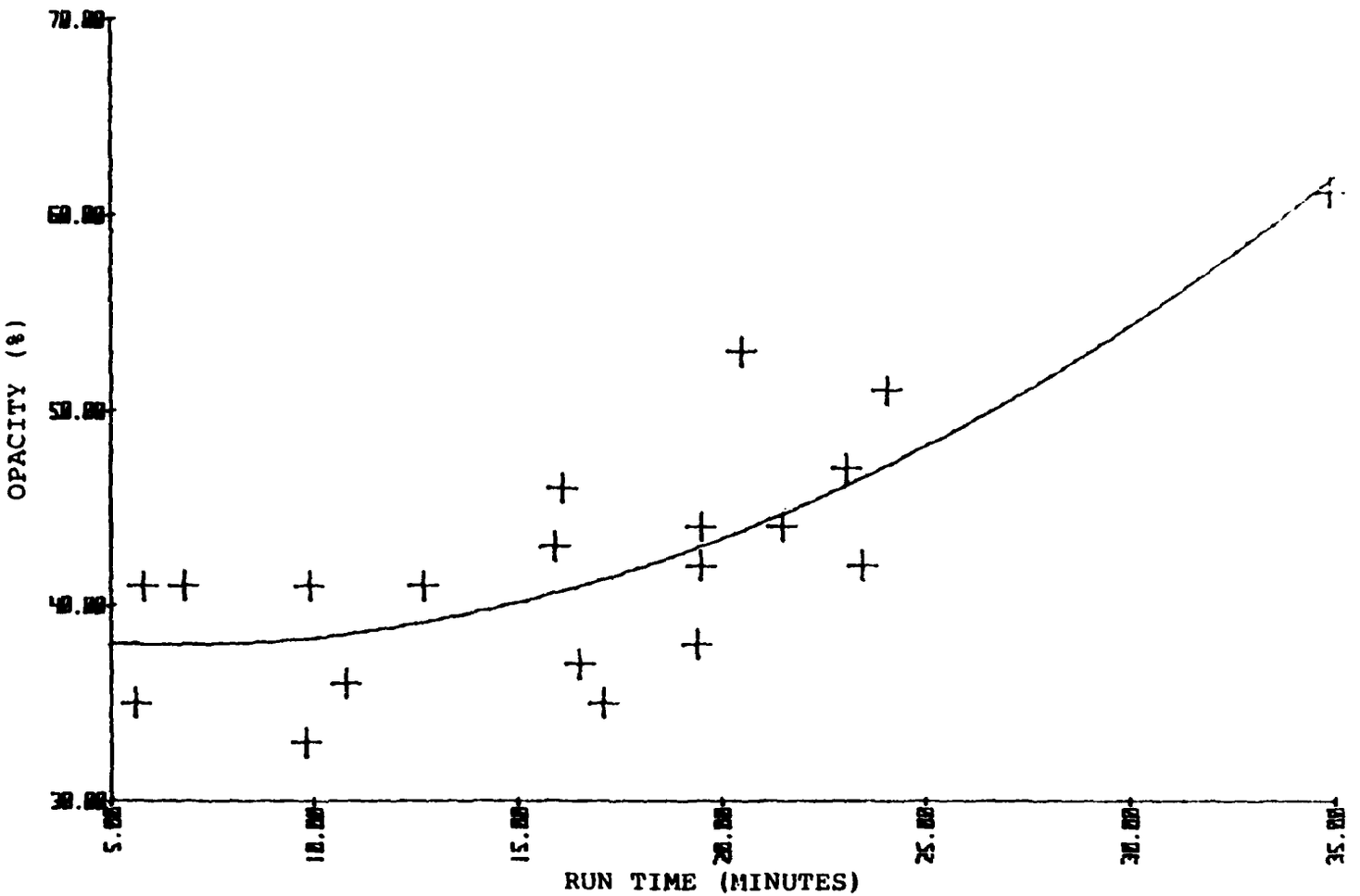

Figure 16. Test Cell Run Time (Starting with Clean Combustor) vs Test Cell Stack Exhaust Gas Opacity

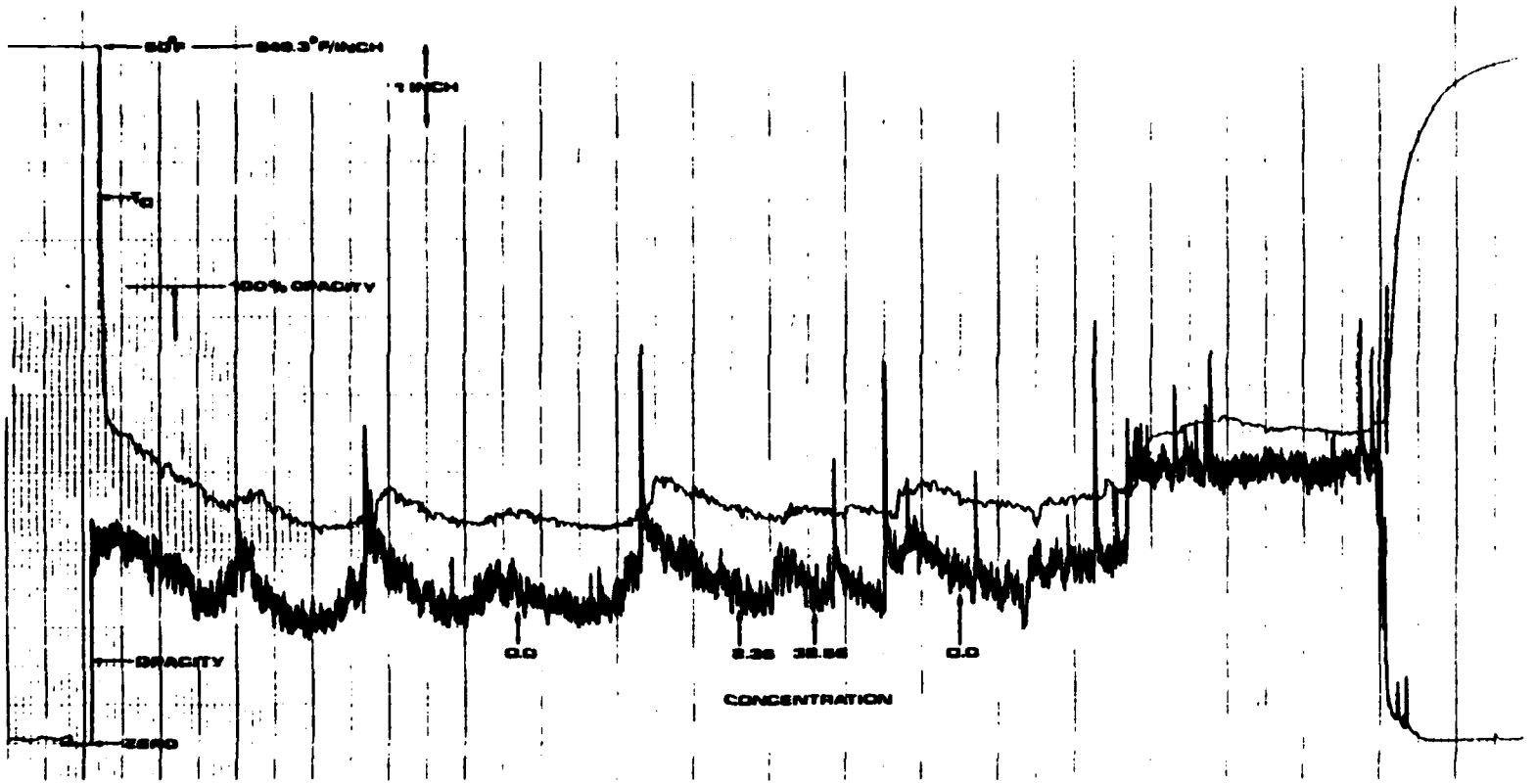

Figure 17. Strip Chart Recording of CV-100 Test Conducted on 16 April 1982 (Combustor Exhaust Temperature (T_C) and Exhaust Gas Opacity, Chart Speed 1 in./min.)

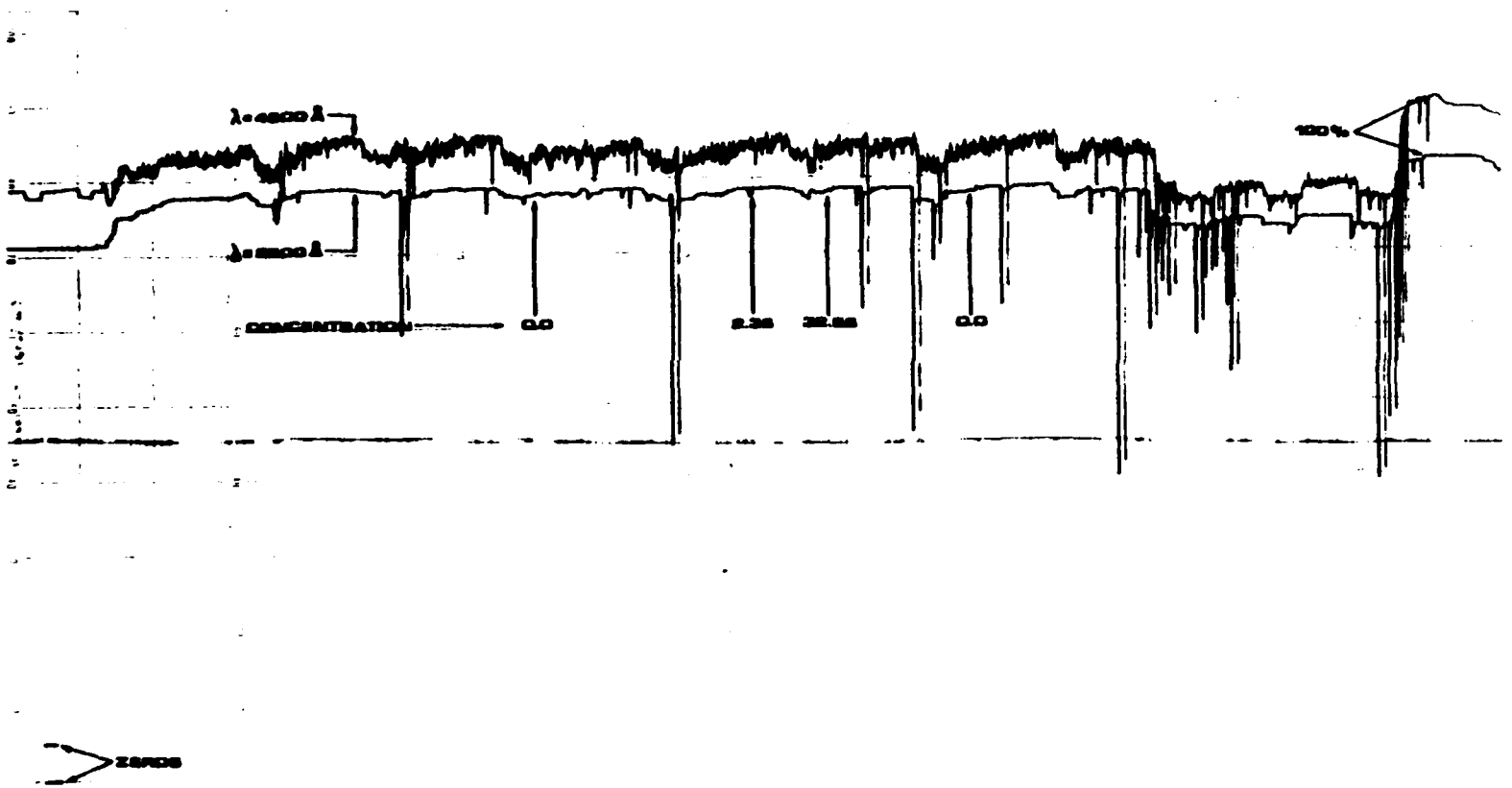

Figure 18. Strip Chart Recording of CV-100 Test Conducted on 16 April 1982 (Engine Exhaust λ = 4500 Å and λ = 6500 Å, Chart Speed 1 in./min.)

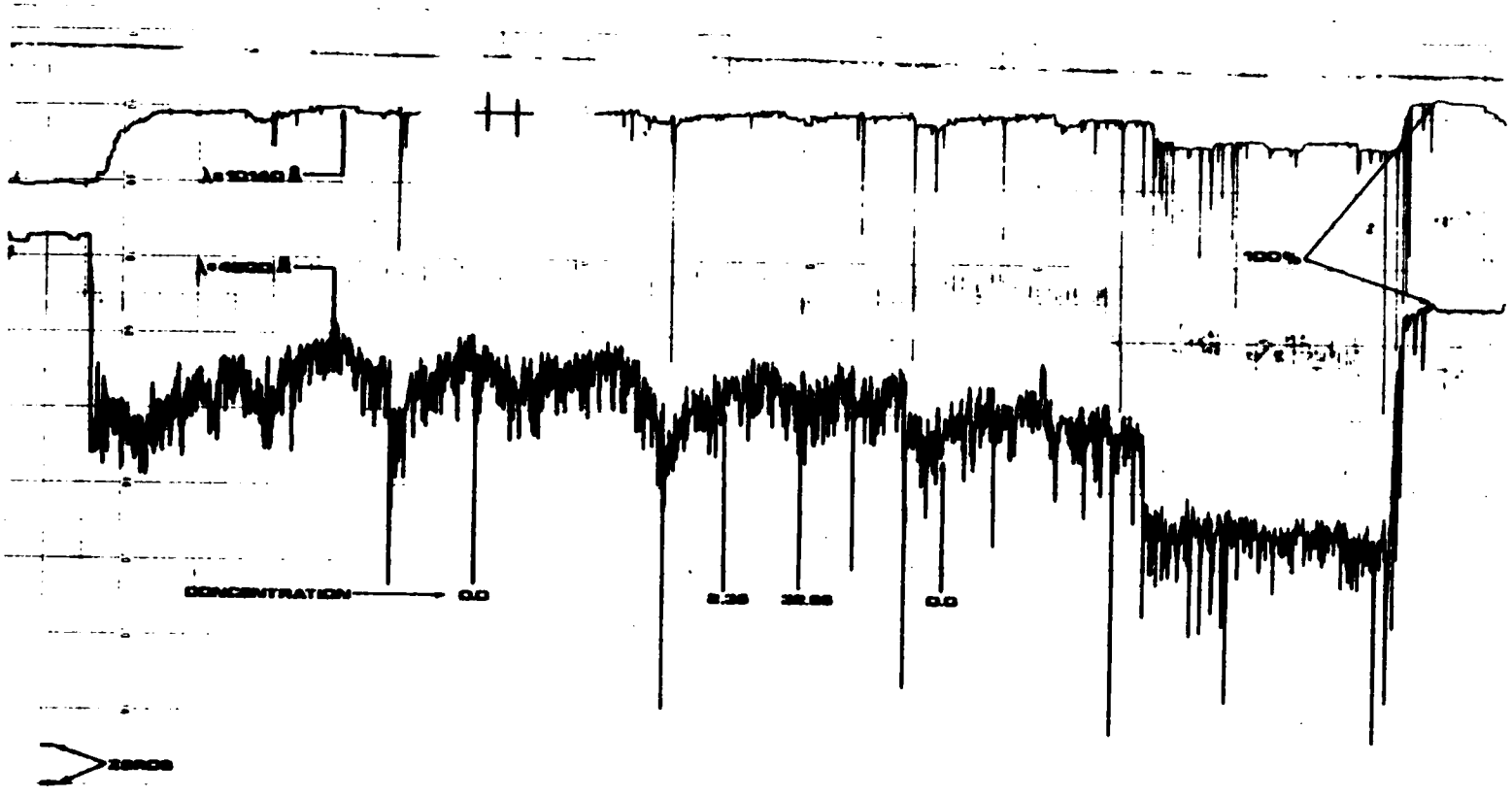

Figure 19. Strip Chart Recording of CV-100 Test Conducted on 16 April 1982 (Engine Exhaust λ = 10140 Å, Stack Exhaust λ = 4500 Å, Chart Speed 1 in./min.)

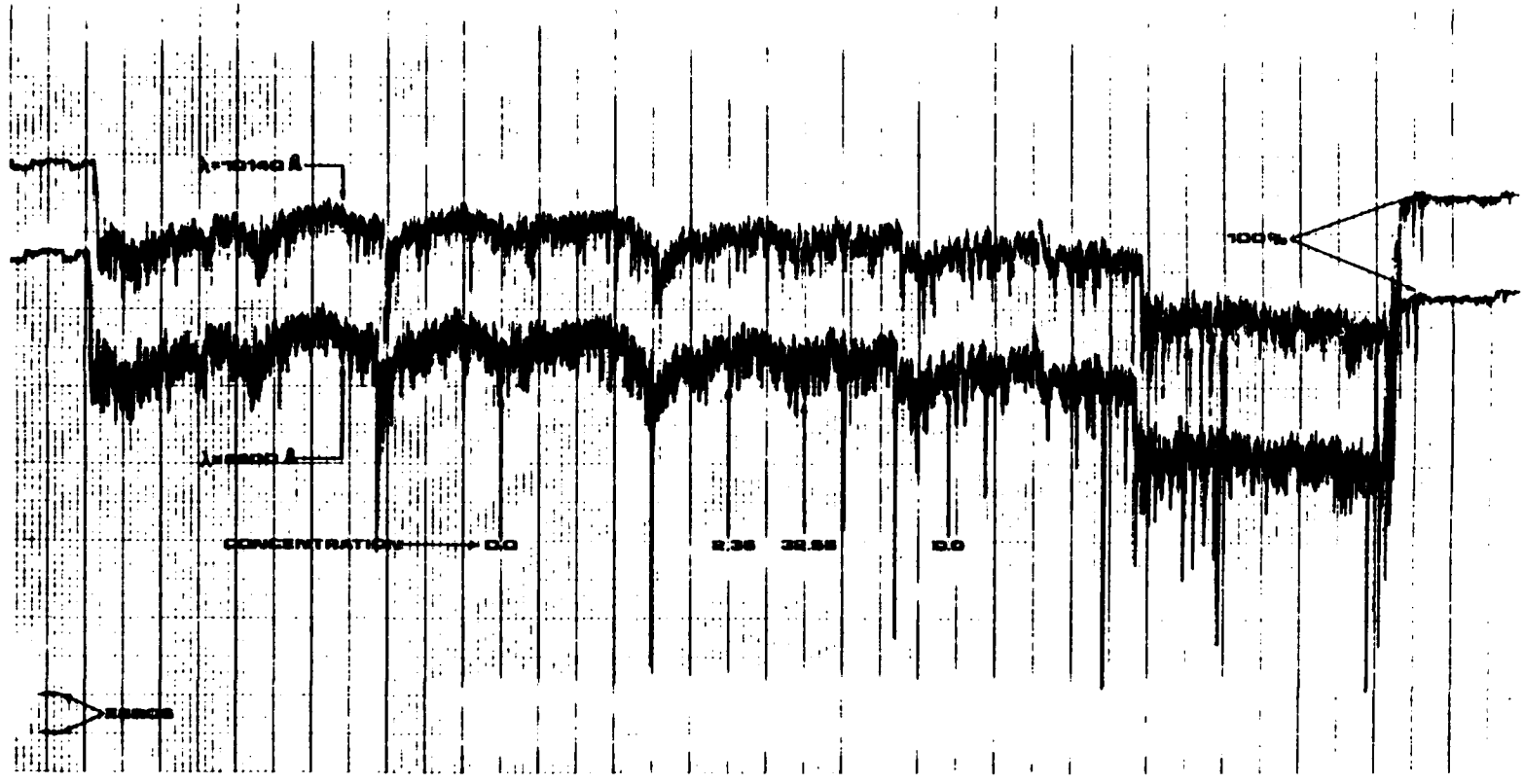

Figure 20. Strip Chart Recording of CV-100 Test Conducted on 16 April 1982 (Stack Exhaust λ = 6500 Å and λ = 10140 Å, Chart Speed 1 in./min.)

Figure 21. SEM Photograph of Engine Exhaust Particulate Sample Collected on 14 May 1982 During Tests with JP-4 Only. (10 Kx Magnification)

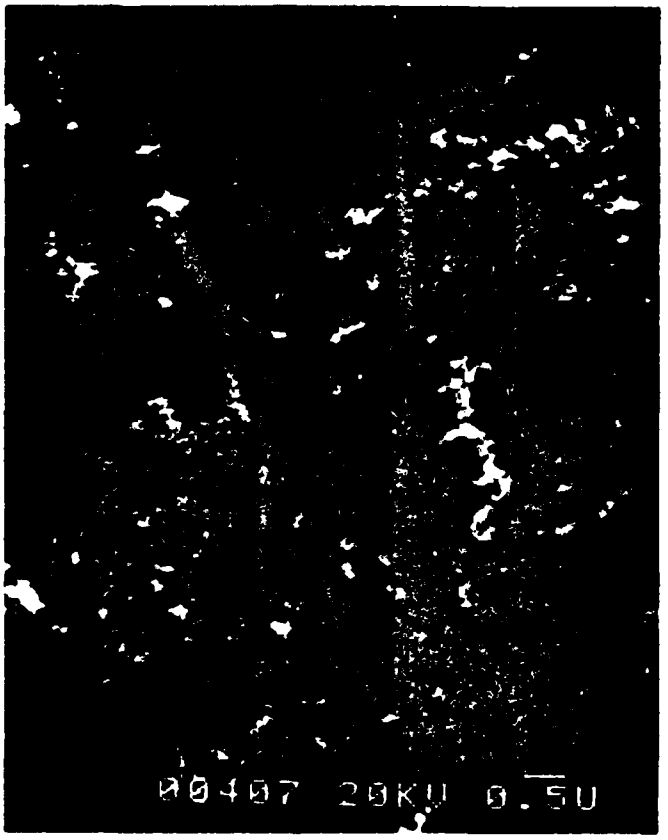

Figure 22. SEM Photograph of Engine Exhaust Particulate Sample Collected on 14 May 1982 During Tests with DGT-2 Concentration of 27.35 ml. additive/gal. JP-4. (10 Kx Magnification)

LIST OF REFERENCES

1. People of the State of California versus Department of the Navy, Civil Case No. C-76-0045 WHO, United States District Court for the Northern District of California of January 1976.

2. Hewlett, H. W., Design, Construction and Testing of a Sub-Scale Turbojet Test Cell, M.S.A.E. Thesis, Naval Postgraduate School, Monterey, California, 1977.

3. Charest, J. R., Combustor Design and Operation for a Sub-Scale Turbojet Test Cell, M.S.A.E. Thesis, Naval Postgraduate School, Monterey, California, 1978.

4. Hewett, M. E., Application of Light Extinction Measurements to the Study of Combustion in Solid Fuel Ramjets, M.S.A.E. Thesis, Naval Postgraduate School, Monterey, California, 1978.

5. Darnell, T. R., Effects of Fuel Additives on Plume Opacity of a Sub-Scale Turbojet Test Cell with a Ramjet Type Dump-Combustor, M.S.A.E. Thesis, Naval Postgraduate School, Monterey, California, 1979.

6. Thornburg, D. W., An Investigation of Engine and Test Cell Operating Conditions on the Effectiveness of Smoke Suppressant Fuel Additives, M.S.A.E. Thesis, Naval Postgraduate School, Monterey, California, 1981.

7. Naval Air Propulsion Test Center, Report No. NAPTC-PE-103, Evaluation of Smoke Suppressant Fuel Additives for Jet Engine Test Cell Smoke Abatement, by A. F. Klarman, February 1977.

8. Naval Environmental Protection Support Service, Report No. AESO 111-72-2, Particulate Emissions from J79, J52, J57, TF30, and TF41 Engines During Test Cell Ferrocene Evaluation, February 1977.

9. Naval Air Propulsion Test Center, Evaluation of the Extended Use of Ferrocene for Test Cell Smoke Abatement; Engine and Environmental Test Results, by A. F. Klarman, October 1971.

10. United Aircraft Research Laboratories, Technical Report No. AFWL-TR-73-18, Analysis of Jet Engine Test Cell Pollution Abatement Methods, by F. L. Robson, A. S. Keston, R. D. Lessard, May 1973.

11. Naval Postgraduate School Report No. NPS-67-82-004, An Investigation of the Effects of Smoke Suppressant Fuel Additives on Engine and Test Cell Exhaust Gas Opacities, by D. W. Thornburg, T. R. Darnell, D. W. Netzer, May 1982.

12. Naval Postgraduate School Report No. 67Nt-77-091, A Sub-Scale Turbojet Test Cell for Design Evaluations and Analytical Model Validation, by H. W. Hewlett, P. J. Hickey, D. W. Netzer, September 1977.

13. The American Society of Mechanical Engineers (ASME) PTC 19.5; 4, Flow Measurement, Instruments and Apparatus, United Engineering Center, 345 East 47th, New York, 1959.

14. Cashdollar, K. L., Lee, C. K., and Singer, J. M., "Three-Wavelength Light Transmission Technique to Measure Smoke Particle Size and Concentration," Applied Optics, Volume 18, Number 11, June 1979.

15. Dobbins, R. A., and Jizmagian, G. S., "Optical Scattering Cross Sections for Polydispersions of Dielectric Spheres," Journal of the Optical Society of America, Vol. 56, No. 10, October 1966, pp. 1345-1354.

16. Monitor Labs, Incorporated, Document 8440E, Instruction Manual Nitrogen Oxides Analyzer Model 8440E, 4202 Sorrento Valley Boulevard, San Diego, California, August 9, 1977.

17. Naval Environmental Support Service, Report No. AESO 161.1-1-76, Field Evaluation of Instruments for the Determination of Smoke Opacity, September 1976.

18. Pagni, P. J., Hughes, L., and Novakov, T., "Smoke Suppressant Additive Effects on Particulate Emissions from Gas Turbine Combustors," AGARD Conference No. 125, Atmospheric Pollution by Aircraft Engines, AGARD-CP-125, 1973.

19. Air Force Engineering and Service Center, Report No. ESL-TR-79-32, Soot Control by Fuel Additives--A Review, by Howard, J. B., and Kausch, W. T., September 1974.

INITIAL DISTRIBUTION LIST

		NO. OF COPIES
1.	Library Code, 0142 Naval Postgraduate School Monterey, CA 93940	2
2.	Department of Aeronautics Code 67 Naval Postgraduate School Monterey, CA 93940	
	Chairman	1
	D. W. Netzer	10
	D. W. Thornburg	2
	J. R. Bramer	2
3.	Dean of Research Code 012 Naval Postgraduate School Monterey, CA 93940	1
4.	Defense Technical Information Center Cameron Station Alexandria, VA 22314	2
5.	Chief of Naval Operations Navy Department Washington, DC 20360 (Attn: Code OP451, IP453)	2
6.	Chief of Naval Material Navy Department Washington, DC 20360 (Attn: Codes: 08T241, 044P1)	2
7.	Commander Naval Air Systems Command Washington, DC 20361 (Codes: AIR-01B, 330D, 3407, 4147A, 50184, 5341B, 53645, 536B1)	8
8.	Commanding Officer Naval Air Rework Facility Naval Air Station North Island San Diego, CA 92135 Code: 64270	1
9.	Commander Naval Facilities Engineering Command 200 Stoval Street Alexandria, VA 22332 (Codes: 104, 032B)	2

NO. OF COPIES

10. Naval Construction Battalion Center — 3
Port Hueneme, CA 93043
(Codes: 25, 251, 252)

11. U. S. Naval Academy — 1
Annapolis, MD 21402
(Attn: Prof. J. Williams)

12. Arnold Engineering Development Center — 1
Arnold AFS, TN 37342
(Code: DYR)

13. Air Force Aero Propulsion Laboratory — 1
Wright-Patterson AFB, OH 45433
(Code: SFF)

14. Detachment 1 — 2
(Civil & Environmental Engineering
Division Office)
HQ ADTC (AFSC)
Tyndall AFB, FL 32401
(Code: EV, EVA)

15. Army Aviation Systems Command — 1
P. O. Box 209
St. Louis, MO 63166
(Code: EQP)

16. Eustis Directorate — 1
USA AMR & DL
Ft. Eustis, VA 23604
(Code: SAVDL-EU-TAP)

17. National Aeronautics and Space Admin. — 1
Lewis Research Center
2100 Brookpark Road
Cleveland, OH 44135
(Attn: Mail Stop 60-6 (R. Rudley))

18. Federal Aviation Administration — 1
National Aviation Facility Experimental Ctr.
Atlantic City, NJ 08405

19. Naval Air Propulsion Center — 3
Trenton, NJ 08628
(Code PE 71:AFK)

20. Naval Ocean Support Center — 2
271 Catalina Boulevard
San Diego, CA 92152
(Attn: M. Lepor, M. Harris, Code 5121)

21. Naval Air Rework Facility — 1
Alameda, CA 94501
ATTN: (G. Evans, Code 642)